

1 **The CHLORAD pathway controls chromoplast development**
2 **and fruit ripening in tomato**

3

4 Qihua Ling^{1,2,3#}, Najiah Mohd. Sadali^{1,4#}, Ziad Soufi¹, Yuan Zhou^{1,2}, Binqun
5 Huang^{1,5}, Yunliu Zeng^{1,6}, Manuel Rodriguez-Concepcion⁷, and R. Paul Jarvis^{1*}

6

7 ¹ Department of Plant Sciences, University of Oxford, Oxford OX1 3RB, UK.

8 ² National Key Laboratory of Plant Molecular Genetics, CAS Center for Excellence in
9 Molecular Plant Sciences, Institute of Plant Physiology and Ecology, Chinese Academy of
10 Sciences, Shanghai, China.

11 ³ CAS-JIC Center of Excellence for Plant and Microbial Sciences (CEPAMS), Institute of
12 Plant Physiology and Ecology, Chinese Academy of Sciences, Shanghai, China.

13 ⁴ Present address: Centre for Research in Biotechnology for Agriculture (CEBAR),
14 University of Malaya, 50603 Kuala Lumpur, Malaysia.

15 ⁵ Present address: School of Agriculture, Yunnan University, Kunming, China.

16 ⁶ Present address: Key Laboratory of Horticultural Plant Biology (Ministry of Education),
17 Huazhong Agricultural University, Wuhan, China.

18 ⁷ Instituto de Biología Molecular y Celular de Plantas (IBMCP), CSIC-Universitat Politècnica
19 de València, 46022 Valencia, Spain.

20 # These authors contributed equally.

21 *To whom correspondence should be addressed: paul.jarvis@plants.ox.ac.uk

22

23

24

25 **Abstract**

26 The maturation of green fleshy fruit to become colourful and flavoursome is an important
27 strategy for plant reproduction and dispersal. In tomato (*Solanum lycopersicum*) and many
28 other species, fruit ripening is intimately linked to the biogenesis of chromoplasts, the
29 plastids that are abundant in ripe fruit and specialized for the accumulation of carotenoid
30 pigments. Chromoplasts develop from pre-existing chloroplasts in the fruit, but the
31 mechanisms underlying this transition are poorly understood. Here, we reveal a role for the
32 CHLORAD proteolytic pathway in chromoplast differentiation. Knockdown of the plastid
33 ubiquitin E3 ligase SP1, or its homologue SPL2, delays tomato fruit ripening, whereas
34 overexpression of SP1 accelerates ripening, as judged by colour changes. We demonstrate
35 that SP1 triggers broader effects on fruit ripening, including fruit softening and gene
36 expression and metabolism changes, by promoting the chloroplast-to-chromoplast transition.
37 Moreover, we show that tomato SP1 and SPL2 regulate leaf senescence, revealing conserved
38 functions of CHLORAD in plants. We conclude that SP1 homologues control plastid
39 transitions during fruit ripening and leaf senescence by enabling reconfiguration of the plastid
40 protein import machinery to effect proteome reorganization. The work highlights the critical
41 role of chromoplasts in fruit ripening, and provides a theoretical basis for engineering crop
42 improvements.

43

44 **Keywords:** plastid, tomato, chromoplast, E3 ligase, fruit ripening, leaf senescence, plastid
45 protein import, ubiquitin-proteasome system, crop improvement

46

47

48 **Main text:**

49 Ripening of fleshy fruits is a complex process that involves dramatic changes in colour,
50 texture, aroma and flavour^{1,2}. The end result is that the fruit becomes an appealing food,
51 attracting animals to help with seed dispersal^{3,4}. Tomato (*Solanum lycopersicum*) is an
52 economically important vegetable, and one of the most well studied models of fleshy fruit
53 ripening.

54 An important component of tomato fruit ripening is the transition of chloroplasts into
55 carotenoid-accumulating plastids termed chromoplasts, which give the red, orange and
56 yellow colours to ripe and ripening tomato fruits^{5,6}. This interconversion process involves the
57 remodelling of the plastid's internal membranes, leading to the formation of carotenoid-rich
58 membranous sacs and the dismantling of thylakoid membranes with concomitant chlorophyll
59 degradation⁶. Such changes are associated with fruit softening, the conversion of starch into
60 simple sugars, and the synthesis of compounds that are associated with taste and aroma; and
61 the overall process is controlled by the hormone ethylene⁷⁻¹⁰. Although chromoplasts are vital
62 constituents of many fleshy fruits, their contribution to fleshy fruit ripening is not well
63 understood. Indeed, the functions of these morphologically complex organelles are far from
64 clear⁶.

65 Chromoplast differentiation is accompanied by, or caused by, major changes in the plastid
66 proteome⁶. Tomato proteomic studies have shown that proteins related to photosynthesis are
67 generally reduced during the chloroplast-to-chromoplast transition, whereas many non-
68 photosynthetic plastid proteins, such as those linked to the biosynthesis of fatty acids, amino
69 acids, carotenoids, vitamins, hormones and aroma volatiles, are accumulated^{7,11-13}. Such
70 changes can be partially attributed to the transcriptional control. For example, genes involved
71 in carotenoid biosynthesis are up-regulated during chromoplast formation^{14,15}, whereas those
72 encoding proteins involved in photosynthesis, such as the major light-harvesting chlorophyll-
73 binding proteins and the small subunit of Rubisco, are down-regulated¹⁶. Nonetheless, post-
74 transcriptional regulation must also have a critical role, as tomato fruit ripening is a rapid
75 process involving dramatic plastid proteome changes, and unneeded proteins must be quickly
76 removed¹⁷. However, in contrast with the role of transcriptional control, the role of post-
77 transcriptional regulation during chromoplast biogenesis is poorly understood¹⁸.

78 An important mechanism underlying the transformation of plastids from one type to another
79 involves direct action of the ubiquitin-proteasome system (UPS), and is mediated by SP1, a

80 RING-type ubiquitin E3 ligase located in the plastid outer envelope membrane¹⁹.
81 Notwithstanding other hypotheses^{20,21}, the SP1 protein was recently shown to operate within
82 a novel pathway for chloroplast protein degradation termed CHLORAD (chloroplast-
83 associated protein degradation)²². The CHLORAD pathway degrades chloroplast outer
84 membrane proteins, including components of the protein import machinery. Numerous
85 studies on chloroplasts have demonstrated the importance of this import machinery,
86 consisting of TOC and TIC (translocons at the outer and inner envelope membranes of
87 chloroplasts), for plastid biogenesis²³⁻²⁷. Significantly, components of the TOC/TIC apparatus
88 have been detected in tomato fruit chromoplasts⁷, indicating that the protein import system is
89 active in chromoplasts. In contrast, proteins associated with internal protein trafficking to the
90 thylakoids are absent¹⁶. These observations point to a need for the active adjustment of
91 protein translocation systems to meet the changing proteomic demands of the organelle.

92 In higher plants like *Arabidopsis*, pea and tomato, TOC receptors exist in different isoforms
93 enabling the formation of substrate-specific translocons and the operation of substrate-
94 specific protein import pathways^{23,25,28}. This may help to meet the requirement for different
95 proteomes in different plastid types, as the overwhelming majority of plastid proteins are
96 imported from the cytosol. This hypothesis has been supported by studies on SP1 in
97 *Arabidopsis*: SP1 regulates chloroplast protein import by selectively targeting TOC
98 components for degradation by the proteasome; and this ultimately controls the plastid
99 proteome and plastid development, which are important during developmental transitions
100 such as de-etiolation and leaf senescence¹⁹. We hypothesized that another important
101 developmental process, the chloroplast-to-chromoplast interconversion, may also be
102 governed by SP1 and protein import, and that this may in turn be crucial for fruit ripening. To
103 address these questions, which cannot be investigated in *Arabidopsis* due to the lack of
104 chromoplasts, we conducted detailed analyses of tomato plants with altered expression of two
105 tomato SP1 homologues, SP1 and SPL2 (SP1-Like2). We show that both E3 ligases play an
106 important role during fruit ripening by regulating TOC components, chromoplast
107 differentiation, and fruit metabolism, and thereby highlight a critical role for post-
108 transcriptional control of plastid proteins during fruit ripening.

109

110 **Results**

111 **Identification and analysis of the localization and expression of tomato SP1 and SPL2**

112 By protein BLAST search analysis, we identified two SP1 homologues in tomato (*Solanum*
113 *lycopersicum*), which we designated sISP1 (Solyc06g084360) and sISPL2 (SP1-Like2,
114 Solyc12g049330) according to an established nomenclature¹⁹. Like *Arabidopsis* SP1 (and its
115 paralogue SPL2), both tomato homologues are predicted to have two transmembrane domains
116 and a highly-conserved C3HC4-type RING finger (RNF) domain (Fig. 1a,b). Overall, the two
117 proteins share 73.3% (sISP1) and 22.1% (sISPL2) amino acid sequence identity with
118 *Arabidopsis* SP1, and 18.5% identity with each other; in fact, sISPL2 is substantially more
119 similar to the *Arabidopsis* SPL2 protein (47.1% identity). Thus, we conclude that sISP1 and
120 sISPL2 are orthologues of *Arabidopsis* SP1 and SPL2, respectively. The moderate sequence
121 divergence between the *Arabidopsis* and tomato orthologues implies that they may have
122 evolved specific functions in the different species.

123 To shed light on the functions of sISP1 and sISPL2, we first investigated their subcellular
124 locations and gene expression profiles. Confocal microscopy analysis of translational fusions
125 to yellow fluorescent protein (YFP) indicated that both sISP1 and sISPL2 are localized at the
126 chloroplast envelope in tomato mesophyll protoplasts (Fig. 1c), which is entirely in line with
127 expectations based on what is known about their counterparts in *Arabidopsis*¹⁹. These data
128 point to a conserved role for sISP1 and sISPL2 in the plastids. While the *sISPL2* gene shows a
129 relatively low and uniform pattern of expression, *sISP1* is highly expressed in meristematic
130 tissues, leaves, ripening fruit, and late stages of development (Fig. 1d, Extended Data Fig. 1);
131 the latter points suggested important roles for *sISP1* in fruit ripening and senescence.

132 **Tomato SP1 homologues function in both dark-induced and ageing-related leaf** 133 **senescence**

134 To investigate the function of sISP1, we generated stable transgenic tomato plants (cv. Ailsa
135 Craig) with altered *sISP1* expression. We employed both artificial microRNA knockdown
136 (KD) and overexpression (OX) driven by the strong 35S promoter, and generated
137 transformed plants via regeneration from *Agrobacterium*-inoculated tomato leaf explants. The
138 efficiency of *sISP1* KD and *sISP1* OX in the transgenic plants was tested by quantitative RT-
139 PCR in the T2 and T3 generations, using wild-type plants also obtained through regeneration
140 as controls. We selected for analysis three independent KD lines in which *sISP1* expression
141 was reduced to ~20% of the wild-type level, and three independent OX lines in which *sISP1*

142 expression was increased >5-fold relative to wild type (Extended Data Fig. 2). For simplicity,
143 in all subsequent analyses we combined the data from the individual KD and OX lines, as
144 they gave similar results. Like the *Arabidopsis* SP1 mutant and OX plants¹⁹, neither slSP1-
145 KD nor slSP1-OX tomato plants were distinguishable from wild type during early vegetative
146 growth suggesting that slSP1 may have special roles in developmental transitions, similar to
147 the *Arabidopsis* protein¹⁹. To investigate this possibility, we began by analysing the tomato
148 transgenics with respect to leaf senescence, during which chloroplasts transition into
149 gerontoplasts⁵.

150 First, we studied premature leaf senescence induced by dark treatment of individual leaves, as
151 was done previously with *Arabidopsis* plants¹⁹. In this experiment, the slSP1-KD leaves
152 remained greener and healthier than wild-type leaves, with no obvious signs of senescence,
153 whereas the slSP1-OX plants showed much more pronounced leaf yellowing than wild-type
154 plants, providing a clear indication of accelerated leaf senescence (Fig. 2a). These visible
155 phenotypes were quantified by measuring chlorophyll contents, which confirmed that slSP1-
156 KD ($p < 0.0001$) and slSP1-OX ($p < 0.001$) leaves retained more and less chlorophyll,
157 respectively, relative to wild type after dark treatment (Fig. 2b). Moreover, photosynthetic
158 performance (as assessed using average, whole-leaf F_v/F_m values determined from
159 chlorophyll fluorescence images) was highest in slSP1-KD leaves, and lowest in the slSP1-
160 OX leaves, indicating accelerated senescence (Fig. 2c). Thus, these results indicated that
161 slSP1 is involved in leaf senescence, revealing conservation of an SP1 function seen
162 previously in *Arabidopsis*.

163 While *Arabidopsis* SP1 was shown to influence dark-induced leaf senescence¹⁹, it was not
164 reported to affect natural, aging-related leaf senescence. Senescence linked to aging might be
165 more significant in large plants like tomato, because such plants typically shed lower leaves
166 as the plant grows, and this process involves senescence of the photosynthetically ineffective
167 leaves to retrieve nutrients. To investigate the role of SP1 in such recurrent leaf senescence,
168 we assessed the leaf aging process in normally growing tomato plants. Although the rate of
169 chlorophyll loss was slower in this analysis, similar trends between the genotypes were
170 eventually observed: measurements showed that the smallest chlorophyll content reduction
171 occurred in the slSP1-KD leaves ($p < 0.0001$), while slSP1-OX leaves experienced the largest
172 change ($p < 0.01$) (Fig. 2d). The photosynthetic performance data not only matched the
173 chlorophyll content data, but also showed that the reduction in F_v/F_m was greatest in the basal
174 leaf margins, most noticeably in slSP1-OX leaves ($p < 0.001$) (Fig. 2e,f). The latter

175 phenomenon is consistent with previous reports suggesting that natural leaf senescence
176 progresses via a coordinated process across the leaf, starting from the tip and edge of the
177 lamina²⁹.

178 Next, to investigate whether *slSPL2* similarly has conserved functions, related to those
179 reported previously for *SP1* in *Arabidopsis*, we generated *slSPL2*-KD transgenic tomato
180 plants, and selected lines showing less than 20% of the wild-type expression level for further
181 analysis (Extended Data Fig. 2). As with the *slSP1* transgenics, we analysed the *slSPL2*-KD
182 lines with respect to dark-induced leaf senescence, measuring wild-type and *slSP1*-KD plants
183 alongside as controls. We found that *slSPL2*-KD leaves also show delayed senescence, as
184 indicated by their greener, healthier appearance due to reduced chlorophyll content loss ($p <$
185 0.05) (Fig. 2g), and their higher photosynthetic performance (F_v/F_m) ($p < 0.0001$) (Fig. 2h,i),
186 relative to wild-type plants. In fact, *slSPL2*-KD had an even stronger effect on senescence
187 than *slSP1*-KD, which is remarkable given that *slSPL2* is normally expressed at much lower
188 levels than *slSP1* ($p < 0.01$) (Fig. 1d), and much less closely related to *Arabidopsis* *SP1*.
189 Overall, these data revealed an important new role for *slSPL2* in leaf senescence, which,
190 together with the *slSP1* data, pointed to a conserved function of *SP1* homologues in leaf
191 plastid development.

192 **Both *SP1* and *SPL2* control tomato fruit ripening**

193 The *slSP1* gene is up-regulated during fruit ripening, and most highly expressed during the
194 breaker stage when chloroplasts lose their photosynthetic apparatus and transit into
195 carotenoid-accumulating chromoplasts (Fig. 1d, Extended Data Fig. 1). This expression
196 pattern suggested that *slSP1* may also play an important role in tomato fruit ripening. In
197 contrast, the *slSPL2* gene shows quite stable expression throughout tomato development.

198 Tomato fruit ripening can be divided into different stages by colour changes, which are
199 successively called mature green, breaker, turning, pink, light red, and red stages³⁰. To
200 investigate potential roles for *SP1* and *SPL2* during fruit ripening, transgenic fruits were
201 harvested at the onset of the breaker stage (at ~36 days post anthesis) and incubated at 25°C
202 in the dark. Detached fruit picked at the breaker stage can be ripened in a controlled way that
203 avoids various environmental changes, allowing for a more consistent analysis of fruit
204 ripening³¹. Prior to the breaker stage, all of our transgenic lines developed normal, mature
205 green fruits such that at the point of harvesting there was no variation in fruit size between
206 the genotypes (Extended Data Fig. 3); this indicated that the *SP1* homologues do not

207 influence the early growth of the fruit, which does not involve plastid type interconversions.

208 To precisely follow the ensuing ripening process, we employed a chroma meter, the readings
209 of which (a^*/b^* values) are based on colour and provide an effective parameter for
210 determining the different stages of tomato fruit ripeness^{32,33} (Fig. 3a). Across multiple fruit
211 populations, we consistently observed a significant delay in the change from breaker to pink
212 and red stages, in both *slSP1*-KD and *slSPL2*-KD fruits, relative to wild type; whereas *slSP1*-
213 OX fruit showed a clear acceleration of this change compared to wild-type fruit. On the first
214 day of the experiment (breaker stage; Day 1), all of the fruits looked similarly green (Fig.
215 3a,b). However, by Day 8, clear differences among the genotypes were already apparent:
216 while the wild-type fruit were past the pink stage, fruit of *slSP1*-KD and *slSPL2*-KD lines
217 were at the turning stage only, whereas those of the *slSP1*-OX lines had already reached the
218 light red stage (Fig. 3a,b). Although the fruits of all the lines eventually reached the red stage
219 (Fig. 3a,b), those of the *slSP1*-KD and *slSPL2*-KD lines took ~23% longer to do so than
220 wild-type fruit, whereas *slSP1*-OX fruit took ~27% less time than wild-type fruit to reach the
221 red stage (Fig. 3a). These results clearly demonstrate that *slSP1* and *slSPL2* both play an
222 important role in tomato fruit ripening, particularly in relation to colour change.

223 It is interesting to note that the *slSPL2*-KD lines displayed a delay in fruit ripening that was
224 broadly similar to that seen in the *slSP1*-KD lines. Together with the observed effect of
225 *slSPL2*-KD on leaf senescence, described above, this supports the notion that *slSPL2* plays a
226 role in plastid transitions that is similarly important to that of *slSP1*.

227 **SP1 controls chromoplast differentiation during tomato fruit ripening**

228 As mentioned earlier, the ripening of fleshy fruits involves systematic changes in a variety of
229 parameters including fruit colour, texture and aroma. Colour changes in particular are closely
230 connected to chromoplast differentiation. In *Arabidopsis*, SP1 is critical for chloroplast
231 development due to its role in regulating the plastid proteome through protein import
232 control¹⁹. Because chromoplast differentiation also involves major changes in the plastid
233 proteome^{11,12,34}, we hypothesized that *slSP1* is important for the efficient differentiation of
234 chloroplasts into chromoplasts. To directly investigate this possibility, fruit from wild-type,
235 *slSP1*-KD and *slSP1*-OX plants collected at the Day 8 post-breaker stage were analysed by
236 transmission electron microscopy (TEM), to study plastid ultrastructure, using fruits at the
237 green and red stages as controls (Fig. 4). Our decision to focus on Day 8 was based on the
238 fact that the most extensive, between-genotype colour differences were apparent at this stage

239 (Fig. 3). For consistency, we analysed only mesocarp (the middle layer of the pericarp) near
240 the base of the fruit, in all cases.

241 At the green stage, wild-type fruit contained typical chloroplasts characterized by the
242 presence of well-developed thylakoid membranes, which either formed stacks known as
243 grana, or simple, interconnecting lamellae (Fig. 4a). At Day 8, when wild-type fruit had
244 reached the pink stage, a majority of the chloroplasts had transformed into immature
245 chromoplasts (Fig. 4a); these are called globular chromoplasts as they possess large
246 plastoglobules (lipid droplets) for accumulating pigments, but they still contain rudimentary
247 remnants of the thylakoid membranes. In wild-type fruit that had reached the red stage, the
248 plastids had completed their differentiation into mature chromoplasts of the type typically
249 found in ripe tomato fruit (Fig. 4a); these are called crystalloid chromoplasts, and they feature
250 large plastoglobules and undulating-shaped envelopes that are shrunken due to the loss of
251 lycopene crystals during the dehydration step of TEM sample preparation¹⁷.

252 Although the slSP1-KD and slSP1-OX samples both displayed a rather homogeneous
253 population of wild-type-like chloroplasts or chromoplasts, respectively at the green and red
254 stages, their plastid populations in fruits at Day 8 showed striking differences (Fig. 4a), all of
255 which accords well with the fruit colour observations (Fig. 3b). Most plastids in Day 8 fruit
256 from slSP1-KD plants contained a relatively intact thylakoid network and few large globular
257 structures, essentially retaining chloroplast features; in contrast, those from slSP1-OX plants
258 had differentiated into typical mature chromoplasts, characterized by undulating membranes
259 and loss of thylakoid structures (Fig. 4a). These trends in the Day 8 fruits were confirmed
260 when the plastids were classified into different developmental stages (chloroplast, immature
261 chromoplast, mature chromoplast) and counted (Fig. 4b); and when the numbers of thylakoid
262 membranes and the sizes of plastoglobules were quantified ($p < 0.0001$ in all cases) (Fig.
263 4c,d). Altogether, these observations clearly showed that chromoplast differentiation was
264 delayed in slSP1-KD fruit and accelerated slSP1-OX fruit, corresponding in both cases with
265 the visible colour differences seen in the fruit (Fig. 3).

266 **SP1 also influences tomato fruit softening and transcriptional reprogramming**

267 Given that SP1 is a plastid-localized regulator, it is not difficult to imagine how it might
268 regulate both chromoplast development and fruit colour, as the latter is directly controlled by
269 the former. However, whether the chromoplast changes mediated by SP1 (or indeed any other
270 factor) can in turn alter aspects of fruit ripening that are not obviously linked to plastids was

271 an interesting open question.

272 To address this issue, we measured the firmness of the ripening tomato fruit using a
273 durometer. Reduction of firmness, or softening, is an important component of fruit ripening
274 controlled by water accumulation, solute metabolism, and cell wall modification, and it is a
275 major fruit quality trait³⁰. As expected, the tomato fruits became much softer at the red stage
276 than those at the breaker stage, in all genotypes (Extended Data Fig. 4a). At these two defined
277 stages, no obvious differences in fruit firmness were observed between the wild-type, slSP1-
278 KD and slSP1-OX plants, which is consistent with the visible fruit phenotypes (Fig. 3).
279 Although fruits of all genotypes still had comparable firmness at the Day 5 post-breaker stage,
280 clear differences became apparent when fruit firmness was measured at later time-points (i.e.,
281 Days 9, 12 and 14 post-breaker) (Extended Data Fig. 4b). In general, slSP1-KD fruit showed
282 significant delays in softening relative to wild-type fruit, whereas slSP1-OX displayed
283 accelerated softening compared to the wild type.

284 It is well known that the fruit ripening process, including softening, is controlled by ethylene-
285 related transcriptional regulation. This affects nuclear genes controlling ethylene synthesis
286 (e.g., *ACO1*, *ACS2*, *ACS4*, *NR*), cell wall degradation (e.g., *PME*, *PG2a*), carotenoid
287 biosynthesis (e.g., *PDS*, *PSY1*), and master transcription factors governing ripening regulators
288 (e.g. *RIN*, *TDR4*)³⁵⁻³⁷. To assess for effects of SP1 on such regulation, we measured the
289 mRNA levels of various genes during tomato fruit development. The results revealed that the
290 differences in colour and softening among wild-type, slSP1-KD and slSP1-OX fruits were
291 accompanied by corresponding changes in expression of ripening-related genes (Extended
292 Data Fig. 5). These results imply that slSP1 regulates fruit softening through transcriptional
293 changes, which are themselves most likely indirect effects of retrograde plastid-to-nucleus
294 signalling during chromoplast development. It is well documented that chloroplasts emit
295 retrograde signals that report on their developmental and functional status in order to regulate
296 nuclear gene expression^{38,39}, and this may even occur during chromoplast biogenesis^{15,40}. We
297 interpret the fruit softening and transcriptional effects of slSP1 to be an example of such
298 regulation.

299 Altogether, these results indicate that SP1 has a comprehensive, holistic effect on fruit
300 ripening that extends beyond direct effects on chromoplast biogenesis, and that chloroplast-
301 to-chromoplast transitions influence the ripening process more generally. This highlights how
302 fruit ripening is orchestrated by remarkably complex controlling pathways.

303 **SP1 influences tomato fruit metabolism**

304 The striking changes in colour during tomato fruit ripening coincide with equally dramatic
305 changes in fruit metabolism, which influence other quality traits such as flavour, nutrition and
306 aroma. As the factories of much metabolism in plants, plastids play a profound role in this
307 process by synthesizing pigments, amino acids, sugars and organic acids⁴¹. To investigate the
308 role of SP1 in orchestrating metabolic changes linked to a plastid type transition, we
309 compared metabolomic profiles of fruit mesocarp from wild-type, slSP1-KD and slSP1-OX
310 plants, at the Day 8 post-breaker and red stages, using both HPLC and GC-MS, and focusing
311 on pigments, sugars, organic acids and amino acids.

312 During the ripening process, tomato fruit accumulate certain carotenoids that are virtually
313 absent from chloroplasts, like lycopene (red) and phytoene, while the levels of
314 photosynthesis-related chlorophylls (green) and xanthophylls such as lutein (yellow) and
315 neoxanthin (yellow) decrease (Fig. 5a)⁴²; these changes underly the change in fruit colour
316 from green (at the breaker stage) to red (at the red stage). As expected based on the fruit
317 colour and plastid morphology data (Fig. 3, 4), all genotypes showed a similar pigment
318 profile at the mature red stage, but differences between the genotypes were clearly apparent
319 at the Day 8 post-breaker stage. The slSP1-KD fruit retained much higher chlorophyll (*a* and
320 *b*) and neoxanthin contents, and more lutein, than wild-type fruit at Day 8, whereas in slSP1-
321 OX fruit the opposite was observed (Fig. 5a). In contrast, slSP1-OX fruit accumulated
322 significantly higher amounts of lycopene and phytoene than wild-type fruit at Day 8, while
323 slSP1-KD hardly accumulated these pigments at all at this stage. Another isoprenoid derivate,
324 tocopherol, was used as a control in this analysis, and this did not vary obviously among
325 these genotypes, indicating that SP1 specifically affects pigment changes during the
326 chloroplast-to-chromoplast transition.

327 Apart from pigments, other major changes in the fruit metabolome during ripening include:
328 the accumulation of certain organic acids, such as caffeic acid and galacturonic acid, and
329 certain amino acids, such as arginine, glutamic acid, and methionine; and, the reduction of
330 certain sugars, such as glycerol, and certain amino acids, such as alanine, glycine, serine and
331 lysine (Fig. 5b)⁴². Interestingly, SP1 may also be required for the proper delivery of these
332 shifts in primary metabolism: such changes appeared delayed in slSP1-KD fruit, and
333 accelerated in slSP1-OX fruit, at the Day 8 post-breaker stage (Fig. 5b). Thus, the data
334 indicate that SP1 is not only required for the metabolism of plastid pigments during tomato

335 fruit development, but in fact it may have a broader role in fruit primary metabolism, most
336 likely through the triggering of the central plastid type change.

337 **SP1 regulates tomato plastid protein levels during plastid transitions**

338 The SP1 E3 ligase was shown to mediate ubiquitination of chloroplast TOC components and
339 their degradation by the UPS to control the chloroplast proteome, and thereby influence the
340 developmental fate and functions of the organelle in *Arabidopsis*^{19,43}. To investigate whether
341 the function of slSP1 is also linked to the control of plastid protein levels, protein extracts
342 from mature, non-senescent leaves of the different tomato genotypes were analysed by
343 immunoblotting (Fig. 6a,b). The data showed that the abundance of Toc75 in slSP1-KD
344 transgenic plants was strongly elevated relative to wild type ($p < 0.001$), and significantly
345 lower in SP1-OX transgenic plants ($p < 0.0001$). In contrast, the levels of Tic40 (which is not
346 a substrate of SP1 in *Arabidopsis*¹⁹) did not change significantly in response to altered
347 expression of *slSP1*. Overall, these data are in agreement with previous results on SP1
348 function in *Arabidopsis*¹⁹, and so support a conserved role of SP1 in regulating TOC proteins
349 in tomato and *Arabidopsis*.

350 Next, to investigate if slSP1 is similarly involved in the plastid proteome changes that occur
351 during leaf senescence and fruit ripening in tomato, protein extracts from whole senescent
352 leaves and the mesocarp of fruits at the Day 8 post-breaker were analysed by
353 immunoblotting. As with the analysis on non-senescent leaves, in both tissues the abundance
354 of Toc75 was strongly increased in slSP1-KD samples, relative to wild type, and reduced in
355 slSP1-OX samples, whereas the abundance of Tic40 was unchanged (Fig. 6c-f). It is
356 noteworthy that the fold change values for Toc75 abundance in slSP1-KD (relative to wild
357 type) in senescent leaves and ripening fruits are larger (> 3 fold) than the value in non-
358 senescent leaves (< 2 fold), as this suggests a particularly important and specific role for
359 slSP1 in controlling plastid protein import during leaf aging and fruit ripening. In line with
360 the results presented earlier showing differences in photosynthetic performance in senescent
361 leaves between the genotypes (Fig. 2e,f), we observed that an important photosystem
362 component (PsbO/OE33) was significantly elevated in slSP1-KD senescent leaves relative to
363 wild type ($p < 0.05$), and slightly reduced in slSP1-OX leaves ($p < 0.05$) (Fig. 6c,d). During
364 tomato fruit ripening, the photosystems are known to decline dramatically¹¹, and,
365 correspondingly, we observed that the abundance of a photosystem component (PsaD)
366 remained higher level in slSP1-KD fruit ($p < 0.05$), and was reduced in slSP1-OX fruit ($p <$

367 0.01) (Fig. 6e,f). In contrast, the amount of a chromoplast marker protein, PGL35, was
368 significantly reduced in slSP1-KD fruit ($p < 0.01$). Altogether, the results support a model in
369 which slSP1 directly degrades the TOC complex to inhibit the import of photosynthetic
370 proteins, which in turn facilitates plastid type transitions during leaf senescence and fruit
371 ripening.

372 Discussion

373 In this study, we identified two chloroplast envelope-localized SP1 homologues in tomato,
374 and showed that they regulate the processes of leaf senescence and fruit ripening.
375 Knockdown of *slSP1* and *slSPL2* expression delayed both leaf senescence and fruit ripening,
376 as judged by visible phenotype, chlorophyll content, photosynthetic performance, plastid
377 ultrastructure, fruit firmness, and metabolism. In contrast, overexpression of *slSP1*
378 accelerated leaf senescence and fruit ripening, according to the same parameters. The
379 consequences of altering *slSP1* expression can be attributed to the regulation of plastid
380 protein import by CHLORAD²², which in turn controls the plastid proteome. Previous work
381 has shown that such regulation is particularly important during developmental stages
382 requiring a plastid type change¹⁹, and leaf senescence and fruit ripening are two such stages;
383 the former involves a chloroplast-to-gerontoplast transition, and the latter a chloroplast-to-
384 chromoplast transition^{5,6}. To date, most molecular analyses of leaf senescence and fruit
385 ripening have been based on mRNA expression^{44,45}, but it is reasonable to assume that other
386 regulatory mechanisms, including protein-level control, are also involved. Indeed, our data
387 point to a critical role for SP1 and the CHLORAD pathway in the regulation of these
388 processes.

389 Previous work in *Arabidopsis* revealed an important role for SP1 in dark-induced leaf
390 senescence, but an effect on aging-related senescence was not observed¹⁹. Here, we found
391 that knockdown of either *slSP1* or *slSPL2* delays both dark-induced and age-related
392 senescence of tomato leaves (Fig. 2). Because different plant species have different
393 senescence physiologies, knowledge gained from one model may not necessarily be
394 applicable to another⁴⁴. One possible reason why SP1 apparently has a relatively more
395 important role in age-related senescence in tomato is that such perennial plants have differing
396 requirements for chloroplast degeneration than annual plants like *Arabidopsis*. Another
397 possibility is that the growth habit of tomato leads to the progressive shading of lower leaves
398 by the canopy above. Thus, SP1 may have even more profound roles in species other than
399 *Arabidopsis*, as the latter is a model plant with relatively simple morphology compared to
400 many other higher plants.

401 The paralogue SPL2 displays similar subcellular localization and domain architecture to SP1,
402 in both tomato and *Arabidopsis* (Fig. 1a-c)¹⁹, suggesting that it may have a similar mode of
403 action to SP1. Nonetheless, the role of SPL2 in *Arabidopsis* has remained unclear^{19,46}. Given

404 that it is one of just a few E3 ligases found in plastids, it is very important to understand its
405 role. Here, we showed that SPL2 and SP1 share conserved functions. Intriguingly,
406 knockdown of *slSPL2* caused a more pronounced effect on leaf senescence than *slSP1*
407 knockdown (Fig. 2g-i), which is surprising given that the mRNA expression of *slSPL2* is
408 much lower than that of *slSP1* (Fig. 1d, Extended Data Fig. 1). This lack of correspondence
409 between phenotypic severity and expression level may reflect differential post-transcriptional
410 regulation of the two components. In *Arabidopsis*, SP1 is subject to proteasomal degradation
411 triggered by self-ubiquitination, which keeps steady-state levels of the protein very low^{19,22}.
412 Thus, lower *slSPL2* mRNA levels do not necessarily mean that *slSPL2* protein levels are
413 lower too. Alternatively, *slSPL2* might have a relatively more potent role in the regulation of
414 leaf senescence, for instance by preferentially targeting plastid components that limit
415 catabolic activity. Indeed, functional differences between *slSP1* and *slSPL2* (e.g., in relation
416 to target specificity) might be expected given that the two proteins share such low sequence
417 similarity, especially in the substrate-binding intermembrane space domain¹⁹. However, the
418 true nature of such functional differences must await further investigation, for example by
419 comparing plants overexpressing *slSP1* or *slSPL2*.

420 Nonetheless, both tomato SP1 homologues play an important role in fruit ripening, as
421 alterations in the expression of either had significant impacts on the speed and duration of
422 fruit ripening: *slSP1-OX* accelerated the process; whereas *slSP1-KD* and *slSPL2-KD* both
423 delayed the process, indicating redundant functions in fruit development (Fig. 3). Fruit
424 ripening is a multifaceted process involving organoleptic changes in colour, flavour, texture
425 and aroma. While these changes occur concomitantly with a dramatic plastid type transition⁶,
426 exactly what the regulatory significance of chromoplast differentiation is within the fruit
427 ripening process has remained poorly explored. The specific role of SP1 in regulating plastid
428 development provided us with a unique opportunity to address this question. First, our TEM
429 results directly showed that SP1 controls plastid type interconversion during fruit
430 development: while wild-type fruit at the post-breaker stage contained predominantly
431 immature chromoplasts with residual characteristics of chloroplasts, *slSP1-KD* and *slSP1-OX*
432 fruit contained mainly typical chloroplasts and mature chromoplasts, respectively (Fig. 4).
433 Then (and most significantly in relation to the question posed above), we found that other
434 aspects of fruit ripening less obviously connected to plastids were also changed, in parallel
435 with the plastid type changes: fruit softening occurred much more slowly and quickly in
436 *slSP1-KD* and *slSP1-OX* fruit, respectively, relative to wild-type fruit (Extended Data Fig.

437 3b); and, the characteristic metabolomic changes that occur between the green and red fruit
438 stages were delayed in slSP1-KD fruit, and accelerated in slSP1-OX fruit (Fig. 5). Thus, the
439 chloroplast-to-chromoplast transition plays a central, controlling role in the ripening process
440 as whole, and is not merely a consequence of the process.

441 As a resident regulator of plastids, SP1 is not likely to control the overall ripening steps
442 directly, given that processes such as fruit softening involve ethylene-induced transcriptional
443 changes in the nucleus⁷⁻¹⁰. However, our data show that the manipulation of slSP1 expression
444 influences a wide range of ripening-related genes involved in processes such as ethylene
445 synthesis and cell wall modification (Extended Data Fig. 5). As chloroplasts are well known
446 to have the ability to modify nuclear gene expression^{38,39}, our results imply that SP1-
447 regulated chromoplast differentiation triggers retrograde signals that help to orchestrate the
448 ripening process. This suggests that the ability to influence nuclear gene expression may be
449 common amongst different plastid types.

450 Transformation of chloroplasts into chromoplasts involves numerous pigment and metabolic
451 changes and the reorganization of the organelle's internal structures, all of which requires
452 extensive reconfiguration of the plastid proteome. To achieve such dramatic proteomic
453 changes in a relatively short time period, one may assume that the timely removal or
454 exclusion of unwanted proteins is critical. Such post-transcriptional regulation is more
455 efficient and quicker than transcriptional control, especially for plastid proteins which require
456 the additional step of protein import. Our previous work demonstrated how SP1 reorganizes
457 the TOC apparatus in *Arabidopsis*¹⁹. In higher plants, TOC receptors exist in different
458 isoforms which enable the formation of substrate-specific translocons and the operation of
459 substrate-specific protein import pathways (e.g., with preference for photosynthesis-related or
460 housekeeping precursor proteins)^{23,25,47}; SP1 modifies the balance between these through
461 selective TOC degradation⁴⁸. The decline in photosynthesis-related proteins during tomato
462 fruit development implies a need for reorganization of the TOC machinery, to accommodate
463 a different set of precursor proteins (e.g., those involved in carotenoid synthesis, lipid
464 metabolism, and chlorophyll catabolism). Thus, slSP1 action may allow for a more rapid fruit
465 ripening process by facilitating plastid proteome changes through TOC reorganization.
466 Consistently, the Toc159 and Toc34 receptor families in tomato comprise isoforms as diverse
467 as those in *Arabidopsis* and pea, implying that similar regulation exists in tomato^{6,28}. Indeed,
468 we observed that the abundance of a photosynthetic protein declines more quickly in slSP1-
469 OX fruit than in wild-type fruit, but remains high in slSP1-KD fruit (Fig. 6). Unfortunately, it

470 was not possible to analyse the TOC receptors themselves because the available antibodies
471 were designed to specifically recognize individual *Arabidopsis* isoforms, and consequently
472 are ineffective in tomato. In the future, it will be interesting to develop a better understanding
473 of the tomato TOC apparatus, and to analyse a greater range of plastid proteins in such
474 experiments, so as to more fully appreciate the dynamics of protein import during fruit
475 ripening in response to slSP1 regulation. Based on the similarities between slSP1-KD and
476 slSPL2-KD plants during leaf senescence and fruit ripening, we can reasonably infer that
477 slSPL2 influences TOC protein levels too.

478 Lastly, it is worth noting that the manipulation of slSP1 or slSPL2 changed the speed of
479 ripening rather than the quality of the fully ripened fruit (as judged in relation to colour, size,
480 firmness, metabolites, and chromoplast ultrastructure). This may reflect the fact that SP1 and
481 SPL2 have partially redundant functions, so that one can compensate for the loss of the other,
482 for example. Alternatively, it may signify that multiple layers of control operate during fruit
483 ripening, so that failure of the SP1/SPL2 pathway may eventually be compensated for by
484 other regulatory systems, such as transcriptional control or different proteolytic pathways.
485 Such redundancy of regulation may, in wild-type fruit, allow for an optimal balance of short-
486 term (post-transcriptional, e.g., via protein import or proteolysis) and long-term
487 (transcriptional) control. This may also explain how green tomato varieties, such as Green
488 Flesh and Green Giant, can still soften and sweeten in spite of the fact that they do not appear
489 to make many chromoplasts⁴⁹. However, differing flesh colour does seem to influence fruit
490 metabolite composition⁵⁰. Regardless, the regulatory properties of SP1 and SPL2 imbue them
491 with significant potential for agricultural use. For example, early and late fruiting varieties of
492 fleshy fruits might be developed; or the transportability and shelf-life of fruit could be
493 improved by delaying ripening without compromising the quality of the ripe fruit.

494

495

- 497 1 Alexander, L. & Grierson, D. Ethylene biosynthesis and action in tomato: a model for
498 climacteric fruit ripening. *J. Exp. Bot.* **53**, 2039-2055 (2002).
- 499 2 Klee, H. J. & Giovannoni, J. J. Genetics and control of tomato fruit ripening and quality
500 attributes. *Annu. Rev. Genet.* **45**, 41-59 (2011).
- 501 3 Seymour, G. B., Ostergaard, L., Chapman, N. H., Knapp, S. & Martin, C. Fruit development
502 and ripening. *Annu. Rev. Plant Biol.* **64**, 219-241 (2013).
- 503 4 Llorente, B., D'Andrea, L. & Rodriguez-Concepcion, M. Evolutionary recycling of light
504 signaling components in fleshy fruits: new insights on the role of pigments to monitor
505 ripening. *Front. Plant Sci.* **7**, 263 (2016).
- 506 5 Jarvis, P. & López-Juez, E. Biogenesis and homeostasis of chloroplasts and other plastids.
507 *Nat. Rev. Mol. Cell Biol.* **14**, 787-802 (2013).
- 508 6 Sadali, N. M., Sowden, R. G., Ling, Q. & Jarvis, R. P. Differentiation of chromoplasts and
509 other plastids in plants. *Plant Cell Rep.* **38**, 803-818 (2019).
- 510 7 Barsan, C. *et al.* Characteristics of the tomato chromoplast revealed by proteomic analysis. *J.*
511 *Exp. Bot.* **61**, 2413-2431 (2010).
- 512 8 Egea, I. *et al.* Chromoplast differentiation: current status and perspectives. *Plant Cell Physiol.*
513 **51**, 1601-1611 (2010).
- 514 9 Li, L. & Yuan, H. Chromoplast biogenesis and carotenoid accumulation. *Arch. Biochem.*
515 *Biophys.* **539**, 102-109 (2013).
- 516 10 Pesaresi, P., Mizzotti, C., Colombo, M. & Masiero, S. Genetic regulation and structural
517 changes during tomato fruit development and ripening. *Front. Plant Sci.* **5**, 124 (2014).
- 518 11 Barsan, C. *et al.* Proteomic analysis of chloroplast-to-chromoplast transition in tomato reveals
519 metabolic shifts coupled with disrupted thylakoid biogenesis machinery and elevated energy-
520 production components. *Plant Physiol.* **160**, 708-725 (2012).
- 521 12 Suzuki, M. *et al.* Plastid proteomic analysis in tomato fruit development. *PLoS One* **10**,
522 e0137266 (2015).
- 523 13 Szymanski, J. *et al.* Label-free deep shotgun proteomics reveals protein dynamics during
524 tomato fruit tissues development. *Plant J.* **90**, 396-417 (2017).
- 525 14 Dalal, M., Chinnusamy, V. & Bansal, K. C. Isolation and functional characterization of
526 lycopene beta-cyclase (CYC-B) promoter from *Solanum habrochaites*. *BMC Plant Biol.* **10**,
527 61 (2010).
- 528 15 Llorente, B. *et al.* Synthetic conversion of leaf chloroplasts into carotenoid-rich plastids
529 reveals mechanistic basis of natural chromoplast development. *Proc. Natl. Acad. Sci. USA*
530 **117**, 21796-21803 (2020).
- 531 16 Pech, J. C., Bouzayen, M. & Latché, A. in *Fruit Ripening: Physiology, Signaling and*
532 *Genomics* (eds P. Nath & M. Bouzayen) 28-47 (CAB International, UK, 2014).
- 533 17 D'Andrea, L. *et al.* Interference with Clp protease impairs carotenoid accumulation during
534 tomato fruit ripening. *J. Exp. Bot.* **69**, 1557-1568 (2018).
- 535 18 D'Andrea, L. & Rodriguez-Concepcion, M. Manipulation of Plastidial Protein Quality
536 Control Components as a New Strategy to Improve Carotenoid Contents in Tomato Fruit.
537 *Front. Plant Sci.* **10**, 1071 (2019).
- 538 19 Ling, Q., Huang, W., Baldwin, A. & Jarvis, P. Chloroplast biogenesis is regulated by direct
539 action of the ubiquitin-proteasome system. *Science* **338**, 655-659 (2012).
- 540 20 Pan, R., Satkovich, J. & Hu, J. E3 ubiquitin ligase SP1 regulates peroxisome biogenesis in
541 *Arabidopsis*. *Proc. Natl. Acad. Sci. USA* **113**, E7307-E7316 (2016).
- 542 21 Ling, Q., Li, N. & Jarvis, P. Chloroplast ubiquitin E3 ligase SP1: does it really function in
543 peroxisomes? *Plant Physiol.* **175**, 586-588 (2017).
- 544 22 Ling, Q. *et al.* Ubiquitin-dependent chloroplast-associated protein degradation in plants.
545 *Science* **363**, eaav4467 (2019).
- 546 23 Jarvis, P. Targeting of nucleus-encoded proteins to chloroplasts in plants (Tansley Review).
547 *New Phytol.* **179**, 257-285 (2008).

- 548 24 Schnell, D. J. The TOC GTPase receptors: regulators of the fidelity, specificity and substrate
549 profiles of the general protein import machinery of chloroplasts. *Protein J.* **38**, 343-350
550 (2019).
- 551 25 Demarsy, E., Lakshmanan, A. M. & Kessler, F. Border control: selectivity of chloroplast
552 protein import and regulation at the TOC-complex. *Front. Plant Sci.* **5**, 483 (2014).
- 553 26 Li, H. M. & Chiu, C. C. Protein transport into chloroplasts. *Annu. Rev. Plant Biol.* **61**, 157-
554 180 (2010).
- 555 27 Shi, L. X. & Theg, S. M. The chloroplast protein import system: from algae to trees. *Biochim.*
556 *Biophys. Acta* **1833**, 314-331 (2013).
- 557 28 Yan, J., Campbell, J. H., Glick, B. R., Smith, M. D. & Liang, Y. Molecular characterization
558 and expression analysis of chloroplast protein import components in tomato (*Solanum*
559 *lycopersicum*). *PLoS One* **9**, e95088 (2014).
- 560 29 Lim, P. O., Kim, H. J. & Nam, H. G. Leaf senescence. *Annu. Rev. Plant Biol.* **58**, 115-136
561 (2007).
- 562 30 Hou, X., Zhang, W., Du, T., Kang, S. & Davies, W. J. Responses of water accumulation and
563 solute metabolism in tomato fruit to water scarcity and implications for main fruit quality
564 variables. *J. Exp. Bot.* **71**, 1249-1264 (2020).
- 565 31 Gray, J. E., Picton, S., Giovannoni, J. J. & Grierson, D. The use of transgenic and naturally
566 occurring mutants to understand and manipulate tomato fruit ripening. *Plant Cell Environ.* **17**,
567 557-571 (1994).
- 568 32 López Camelo, A. F. & Gómez, P. A. Comparison of color indexes for tomato ripening.
569 *Hortic. Bras.* **22**, 534-537 (2004).
- 570 33 Batu, A. Determination of acceptable firmness and colour values of tomatoes. *J. Food Eng.*
571 **61**, 471-475 (2004).
- 572 34 Zeng, Y. *et al.* A comprehensive analysis of chromoplast differentiation reveals complex
573 protein changes associated with plastoglobule biogenesis and remodeling of protein systems
574 in sweet orange flesh. *Plant Physiol.* **168**, 1648-1665 (2015).
- 575 35 Martel, C., Vrebalov, J., Tafelmeyer, P. & Giovannoni, J. J. The tomato MADS-box
576 transcription factor RIPENING INHIBITOR interacts with promoters involved in numerous
577 ripening processes in a COLORLESS NONRIPENING-dependent manner. *Plant Physiol.*
578 **157**, 1568-1579 (2011).
- 579 36 Pan, Y. *et al.* Network inference analysis identifies an APRR2-like gene linked to pigment
580 accumulation in tomato and pepper fruits. *Plant Physiol.* **161**, 1476-1485 (2013).
- 581 37 Rigano, M. M., Lionetti, V., Raiola, A., Bellincampi, D. & Barone, A. Pectic enzymes as
582 potential enhancers of ascorbic acid production through the D-galacturonate pathway in
583 Solanaceae. *Plant Sci.* **266**, 55-63 (2018).
- 584 38 Chan, K. X., Phua, S. Y., Crisp, P., McQuinn, R. & Pogson, B. J. Learning the languages of
585 the chloroplast: retrograde signaling and beyond. *Annu. Rev. Plant Biol.* **67**, 25-53 (2016).
- 586 39 Zhao, X., Huang, J. & Chory, J. Unraveling the linkage between retrograde signaling and
587 RNA metabolism in plants. *Trends Plant Sci.* **25**, 141-147 (2020).
- 588 40 Wu, G. Z. & Bock, R. GUN control in retrograde signaling: How GENOMES UNCOUPLED
589 proteins adjust nuclear gene expression to plastid biogenesis. *Plant Cell*, koaa048 (2021).
- 590 41 Chen, Y. *et al.* Formation and change of chloroplast-located plant metabolites in response to
591 light conditions. *Int. J. Mol. Sci.* **19** (2018).
- 592 42 Carrari, F. *et al.* Integrated analysis of metabolite and transcript levels reveals the metabolic
593 shifts that underlie tomato fruit development and highlight regulatory aspects of metabolic
594 network behavior. *Plant Physiol.* **142**, 1380-1396 (2006).
- 595 43 Ling, Q. & Jarvis, P. Regulation of chloroplast protein import by the ubiquitin E3 ligase SP1
596 is important for stress tolerance in plants. *Curr. Biol.* **25**, 2527-2534 (2015).
- 597 44 Woo, H. R., Kim, H. J., Lim, P. O. & Nam, H. G. Leaf senescence: systems and dynamics
598 aspects. *Annu. Rev. Plant Biol.* **70**, 347-376 (2019).
- 599 45 Wang, R., Angenent, G. C., Seymour, G. & de Maagd, R. A. Revisiting the role of master
600 regulators in tomato ripening. *Trends Plant Sci.* **25**, 291-301 (2020).

601 46 Gao, W., Liu, W., Zhao, M. & Li, W. X. *NERF* encodes a RING E3 ligase important for
602 drought resistance and enhances the expression of its antisense gene *NFYA5* in *Arabidopsis*.
603 *Nucleic Acids Res.* **43**, 607-617 (2015).

604 47 Teng, Y. S., Chan, P. T. & Li, H. M. Differential age-dependent import regulation by signal
605 peptides. *PLoS Biol.* **10**, e1001416 (2012).

606 48 Kessler, F. Plant science. Chloroplast delivery by UPS. *Science* **338**, 622-623 (2012).

607 49 Cheung, A. Y., McNellis, T. & Piekos, B. Maintenance of chloroplast components during
608 chromoplast differentiation in the tomato mutant *green flesh*. *Plant Physiol.* **101**, 1223-1229
609 (1993).

610 50 Dono, G. *et al.* Color mutations alter the biochemical composition in the San Marzano tomato
611 fruit. *Metabolites* **10**, 110 (2020).

612 51 Li, W. *et al.* Genome-wide and functional annotation of human E3 ubiquitin ligases identifies
613 MULAN, a mitochondrial E3 that regulates the organelle's dynamics and signaling. *PLoS*
614 *ONE* **3**, e1487 (2008).

615 52 Parry, C., Blonquist, J. M., Jr. & Bugbee, B. In situ measurement of leaf chlorophyll
616 concentration: analysis of the optical/absolute relationship. *Plant Cell Environ.* **37**, 2508-2520
617 (2014).

618 53 Gálvez-Valdivieso, G. *et al.* The high light response in *Arabidopsis* involves ABA signaling
619 between vascular and bundle sheath cells. *Plant Cell* **21**, 2143-2162 (2009).

620 54 Goodstein, D. M. *et al.* Phytozome: a comparative platform for green plant genomics. *Nucleic*
621 *Acids Res.* **40**, D1178-D1186 (2012).

622 55 Thompson, J. D., Higgins, D. G. & Gibson, T. J. CLUSTAL W: improving the sensitivity of
623 progressive multiple sequence alignment through sequence weighting, position-specific gap
624 penalties and weight matrix choice. *Nucleic Acids Res.* **22**, 4673-4680 (1994).

625 56 Schwacke, R. *et al.* ARAMEMNON, a novel database for *Arabidopsis* integral membrane
626 proteins. *Plant Physiol.* **131**, 16-26 (2003).

627 57 Ossowski, S., Schwab, R. & Weigel, D. Gene silencing in plants using artificial microRNAs
628 and other small RNAs. *Plant J.* **53**, 674-690 (2008).

629 58 Fernandez, A. I. *et al.* Flexible tools for gene expression and silencing in tomato. *Plant*
630 *Physiol.* **151**, 1729-1740 (2009).

631 59 Schwab, R., Ossowski, S., Riester, M., Warthmann, N. & Weigel, D. Highly specific gene
632 silencing by artificial microRNAs in *Arabidopsis*. *Plant Cell* **18**, 1121-1133 (2006).

633 60 Karimi, M., Inze, D. & Depicker, A. GATEWAY vectors for *Agrobacterium*-mediated plant
634 transformation. *Trends Plant Sci.* **7**, 193-195 (2002).

635 61 Chetty, V. J. *et al.* Evaluation of four *Agrobacterium tumefaciens* strains for the genetic
636 transformation of tomato (*Solanum lycopersicum* L.) cultivar Micro-Tom. *Plant Cell Rep* **32**,
637 239-247 (2013).

638 62 Sun, H. J., Uchii, S., Watanabe, S. & Ezura, H. A highly efficient transformation protocol for
639 Micro-Tom, a model cultivar for tomato functional genomics. *Plant Cell Physiol.* **47**, 426-431
640 (2006).

641 63 Koornneef, M. *et al.* Chromosomal instability in cell- and tissue cultures of tomato haploids
642 and diploids. *Euphytica* **43**, 179-186 (1989).

643 64 Karimi, M., De Meyer, B. & Hilson, P. Modular cloning in plant cells. *Trends Plant Sci.* **10**,
644 103-105 (2005).

645 65 Wu, F. H. *et al.* Tape-*Arabidopsis* Sandwich - a simpler *Arabidopsis* protoplast isolation
646 method. *Plant Methods* **5**, 16 (2009).

647 66 Kasmati, A. R., Töpel, M., Patel, R., Murtaza, G. & Jarvis, P. Molecular and genetic analyses
648 of Tic20 homologues in *Arabidopsis thaliana* chloroplasts. *Plant J.* **66**, 877-889 (2011).

649 67 Hobson, G. E., Adams, P. & Dixon, T. J. Assessing the color of tomato fruit during ripening.
650 *J. Sci. Food Agric.* **34**, 286-292 (1983).

651 68 Pathare, P. B., Opara, U. L. & Al-Said, F. A. Colour measurement and analysis in fresh and
652 processed foods: a review. *Food Bioproc. Tech.* **6**, 36-60 (2013).

653 69 Arazuri, S., Jarén, C., Arana, J. I. & de Ciriza, J. P. Influence of mechanical harvest on the
654 physical properties of processing tomato (*Lycopersicon esculentum* Mill.). *J. Food Eng.* **80**,
655 190-198 (2015).

656 70 Walsby-Tickle, J. *et al.* Anion-exchange chromatography mass spectrometry provides
657 extensive coverage of primary metabolic pathways revealing altered metabolism in IDH1
658 mutant cells. *Commun. Biol.* **3**, 247 (2020).

659 71 Liseč, J., Schauer, N., Kopka, J., Willmitzer, L. & Fernie, A. R. Corrigendum: Gas
660 chromatography mass spectrometry-based metabolite profiling in plants. *Nat. Protoc.* **10**,
661 1457 (2015).

662 72 Aronsson, H. *et al.* Nucleotide binding and dimerization at the chloroplast pre-protein import
663 receptor, atToc33, are not essential *in vivo* but do increase import efficiency. *Plant J.* **63**, 297-
664 311 (2010).

665 73 Faurobert, M., Pelpoir, E. & Chaib, J. Phenol extraction of proteins for proteomic studies of
666 recalcitrant plant tissues. *Methods Mol. Biol.* **355**, 9-14 (2007).

667 74 Kovacheva, S. *et al.* *In vivo* studies on the roles of Tic110, Tic40 and Hsp93 during
668 chloroplast protein import. *Plant J.* **41**, 412-428 (2005).

669 75 Kovacheva, S., Bédard, J., Wardle, A., Patel, R. & Jarvis, P. Further *in vivo* studies on the
670 role of the molecular chaperone, Hsp93, in plastid protein import. *Plant J.* **50**, 364-379
671 (2007).

672 76 Huang, W., Ling, Q., Bédard, J., Lilley, K. & Jarvis, P. *In vivo* analyses of the roles of
673 essential Omp85-related proteins in the chloroplast outer envelope membrane. *Plant Physiol.*
674 **157**, 147-159 (2011).

675 77 Suorsa, M. & Aro, E. M. Expression, assembly and auxiliary functions of photosystem II
676 oxygen-evolving proteins in higher plants. *Photosynth Res.* **93**, 89-100 (2007).

677 78 Andersen, B., Koch, B. & Scheller, H. V. Structural and functional analysis of the reducing
678 side of photosystem I. *Physiol. Plant.* **84**, 154-161 (1992).

679 79 Luo, T. *et al.* Distinct carotenoid and flavonoid accumulation in a spontaneous mutant of
680 Ponkan (*Citrus reticulata* Blanco) results in yellowish fruit and enhanced postharvest
681 resistance. *J. Agric. Food Chem.* **63**, 8601-8614 (2015).

682 80 Hruz, T. *et al.* Genevestigator v3: a reference expression database for the meta-analysis of
683 transcriptomes. *Adv. Bioinformatics* **2008**, 420747 (2008).

684

685

686 **Acknowledgements**

687 We are grateful to Errin Johnson and Raman Dhaliwal for transmission electron microscopy
688 conducted in the Sir William Dunn School of Pathology EM Facility, to David Hauton and
689 James McCullagh for IC-MS conducted in the Mass Spectrometry Research Facility in the
690 Department of Chemistry, to Pedro Bota for GC-MS conducted in the Department of Plant
691 Sciences, to Pedro Bota and Rita Ross for technical assistance, and to M. Rosa Rodriguez
692 Goberna for HPLC conducted at CRAG, Spain. This work was supported by a Khazanah-
693 Oxford Centre for Islamic Studies Merdeka Scholarship (to NMS), by Strategic Priority
694 Research Program (Type-B; project number: XDB27040211), Chinese Academy of Sciences
695 (to QL), by the Spanish Agencia Estatal de Investigación (grants BIO2017-84041-P and
696 BIO2017-90877-REDT; to MRC), and by the Biotechnology and Biological Sciences
697 Research Council (BBSRC; grants BB/H008039/1, BB/K018442/1, BB/N006372/1,
698 BB/R005591/1, BB/R009333/1 and BB/R016984/1; to RPJ).

699 **Author contributions**

700 QL and NMS designed and conducted the experiments, analysed the data, and wrote the
701 manuscript. ZS, YZ and BH assisted with the fruit phenotypical analyses, immunoblotting,
702 preparation of samples for the TEM and metabolomic experiments, and data analysis. MRC
703 performed the HPLC analysis of pigments and analysed the results. RPJ conceived of the
704 study, supervised the work, analysed the data, and wrote the manuscript.

705 **Competing interests**

706 The application of CHLORAD as a technology for crop improvement is covered by a patent
707 application.

708

709 **Figure Legends**

710

711 **Fig. 1 | Sequence, localization and gene expression analysis of *slSP1* and *slSPL2*.** **a**,
712 Domain maps illustrating the structural organization of *slSP1* and *slSPL2*. Transmembrane
713 domains (TMD) are shown in red and RING finger domains (RNF) are shown in blue. **b**,
714 Amino acid sequence alignment of the C3HC4-type RNF domains of *Arabidopsis* SP1
715 (At1g63900) and SPL2 (At1g54150), *slSP1* and *slSPL2*, and *Homo sapiens* MULAN
716 (NM_024544), a human mitochondrial outer-membrane protein which controls mitochondrial
717 dynamics⁵¹. Residues conserved in at least three of the four sequences are shaded black. The
718 critical conserved Cys and His residues are indicated with asterisks. **c**, Confocal microscopy
719 images of tomato leaf protoplasts transiently expressing *slSP1*-YFP and *slSPL2*-YFP. The
720 YFP fluorescence signal is shown in green, and chlorophyll autofluorescence is shown in red;
721 an overlay of these two is also shown (Merge). Bright field images confirm the intactness of
722 the protoplasts. Scale bar corresponds to 10 μ m. **d**, Quantitative RT-PCR analysis of *slSP1*
723 and *slSPL2* expression in different tomato organs and at different developmental stages,
724 normalized to the expression of *slACTIN*. Fruit developmental stages analysed were: 0.5 cm
725 diameter developing (0.5 cm), pre-mature green (Pre MG), mature green (MG), breaker, pink,
726 and red. Values are means \pm SEM of 3-6 biological replicates.

727

728 **Fig. 2 | Analyses of the roles of *slSP1* and *slSPL2* in tomato leaf senescence.** **a-c**, Effect of
729 *slSP1* on dark-induced leaf senescence. Individual leaves of 2-month-old wild type (WT),
730 *slSP1* knockdown (KD), and *slSP1* overexpression (OX) tomato plants were covered with
731 aluminium foil for a number of days, as was done previously with *Arabidopsis* plants¹⁹. The
732 leaves were analysed before (Day 1) and after (Day 30) the dark treatment. Representative
733 leaves at Day 30 were photographed (**a**). Leaves were analysed in relation to both:
734 chlorophyll content (**b**) ($n = 12-18$ leaves; **** $p = 0.0001$ [Day 30, KD] and *** $p = 0.0004$
735 [Day 30, OX], compared with WT); and photosynthetic performance (F_v/F_m) (**c**) ($n = 9-10$
736 leaves; **** $p = 0.0001$ [KD] and *** $p = 0.0002$ [OX], compared with WT). Leaves in **c**
737 were analysed on Day 30. **d-f**, Effect of *slSP1* on age-related leaf senescence. The leaves of
738 similar tomato plants growing under standard conditions (i.e., without a dark treatment) were
739 analysed over a more extended time period; Day 1 corresponds to the beginning of the
740 experiment when the plants were 2 months old. Leaves were analysed in relation to both:

741 chlorophyll content (**d**) ($n = 10-20$ leaves; $*p = 0.0462$ [Day 30, KD], $****p = 0.0001$ [Day
742 45, KD], and $**p = 0.0046$ [Day 45, OX], compared with WT); and photosynthetic
743 performance (F_v/F_m) (**e,f**) ($n = 8-10$ leaves; $****p = 0.0001$ [KD] and $***p = 0.0009$ [OX],
744 compared with WT). Leaves in **e** and **f** were analysed on Day 45. A colour spectrum
745 representing the range of F_v/F_m values recorded is shown to the left of the leaf images (**e**),
746 and average values were calculated using the images shown and other similar images (**f**). **g-i**,
747 Effect of *slSPL2* on dark-induced leaf senescence. Individual leaves of 2-month-old WT,
748 *slSPL2*-KD and *slSP1*-KD plants were dark treated as in **a-c** for a number of days.
749 Chlorophyll contents were measured on the same leaf before (Day 1) and after (Day 16) the
750 dark treatment (**g**) ($n = 16-19$ leaves; $****p = 0.0001$ [Day 30, KD] and $****p = 0.0001$ [Day
751 30, OX], compared with WT). Photosynthetic performance (F_v/F_m) was measured on Day 16
752 (**h,i**). A colour spectrum representing the range of F_v/F_m values recorded is shown to the left
753 of the leaf images (**h**), and average values were calculated using the images shown and other
754 similar images (**i**) ($n = 10$ leaves; $****p = 0.0001$ [*slSPL2*-KD] and $****p = 0.0001$ [*slSP1*-
755 KD], compared with WT). All values are means \pm SEM of at least eight experiments. The p
756 values were derived from an unpaired two-tailed Student's t -test; WT was used as the
757 reference group for the statistical analyses.

758

759 **Fig. 3 | Examination of the effects of *slSP1* and *slSPL2* on tomato fruit ripening.** **a**, Fruit
760 from the indicated genotypes were harvested at breaker stage (Day 1) and then monitored
761 daily using a Chroma Meter, all the way through to the mature red stage. How the recorded
762 colour (a^*/b^*) values relate to different stages of fruit ripening is indicated to the right³³. The
763 data shown were derived from fruit populations harvested from two individual T2 generation
764 tomato plants from each of two independent transformants per genotype. Values are means \pm
765 SEM of 30-40 fruits per genotype. **b**, Representative fruit of each genotype from the
766 experiment shown in **a** were photographed at the breaker stage (Day 1), at the Day 8 post-
767 breaker stage, and at the red stage.

768

769 **Fig. 4 | Ultrastructural analysis of the effects of *slSP1* on the chloroplast-to-chromoplast**
770 **transition in ripening tomato fruit.** **a**, Fruit from wild-type (WT), *slSP1*-KD (KD), and
771 *slSP1*-OX (OX) plants at the breaker stage (Day 1), the Day 8 post-breaker stage, and the red
772 (R) stage, were analysed by transmission electron microscopy. Images of representative

773 plastids in each genotype at each stage are shown. Scale bar correspond to 1 μ m. The plastids
774 were classified by their ultrastructure as follows: Stage I (S.I; chloroplast-like), Stage II (S.II;
775 immature chromoplast-like), and Stage III (S.III; mature chromoplast-like). **b-d**, Quantitative
776 data derived from the analysis in **a**. The proportion of plastids at each of the three
777 developmental stages defined above (I, II and III) in fruit at the Day 8 post-breaker stage was
778 determined (**b**) ($n = 3$ tomato lines). Total numbers of thylakoid lamellae per plastid in each
779 genotype at Day 8 were counted (**c**) ($n = 30$ plastids). Diameters of plastoglobules in plastids
780 of each genotype at Day 8 were measured (**d**) ($n = 52$ plastids). All values are means \pm SEM.

781

782 **Fig. 5 | Metabolic profile analyses of the effects of slSP1 on tomato fruit ripening.**

783 Relative metabolite contents of pericarp tissue samples from wild-type (WT), slSP1-KD
784 (KD), and slSP1-OX (OX) fruits at the Day 8 post-breaker (8d) and red stages were
785 determined. **a**, Levels of pigments and derivatives were measured by HPLC, and their relative
786 amounts are shown. Left, carotenoid levels; right, chlorophyll and tocopherol levels ($n = 3-6$
787 samples). **b**, Levels of organic acids, soluble sugars, and amino acids were measured by IC-
788 MS or GC-MS. Histograms show the relative amounts of metabolites typically influenced by
789 fruit ripening ($n = 3-6$ samples). All values are expressed relative to the corresponding value
790 for WT-8d, which in each case is set to 1. Values are means \pm SEM.

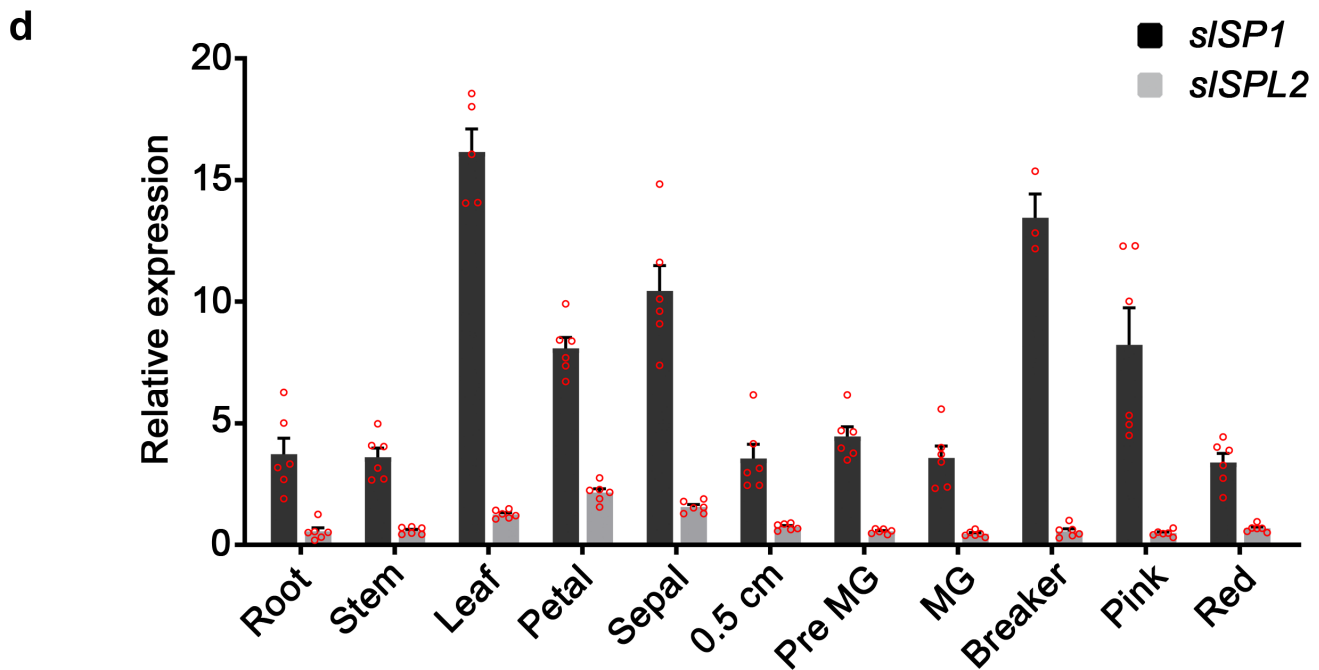
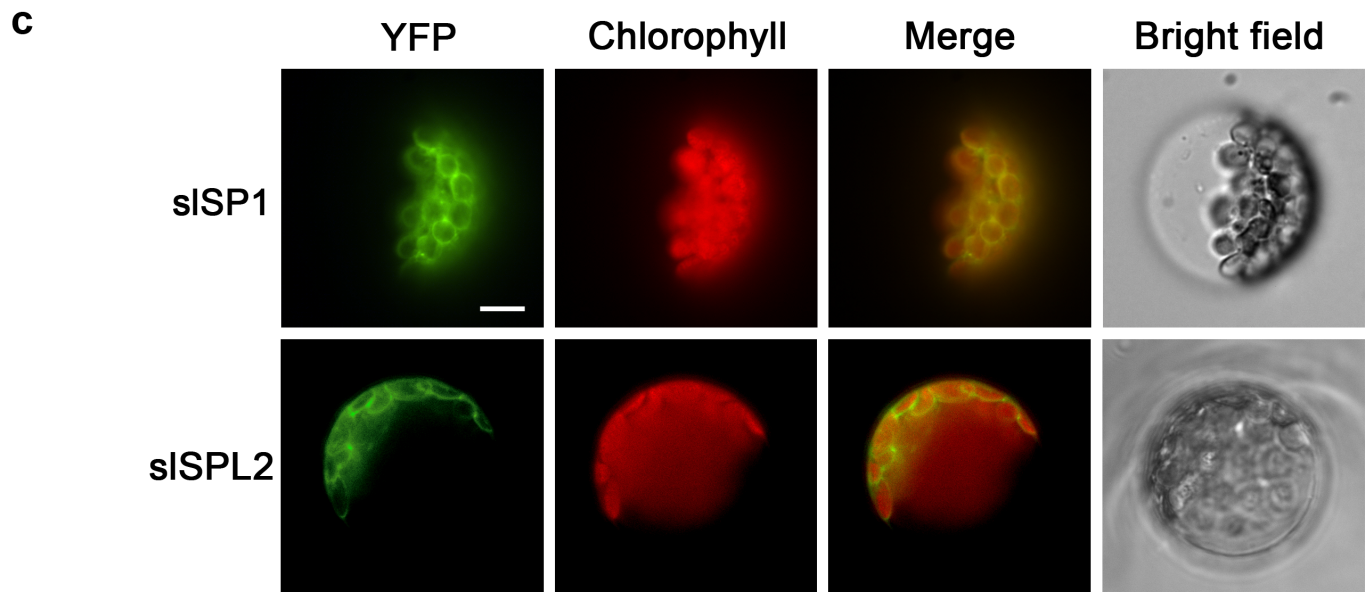
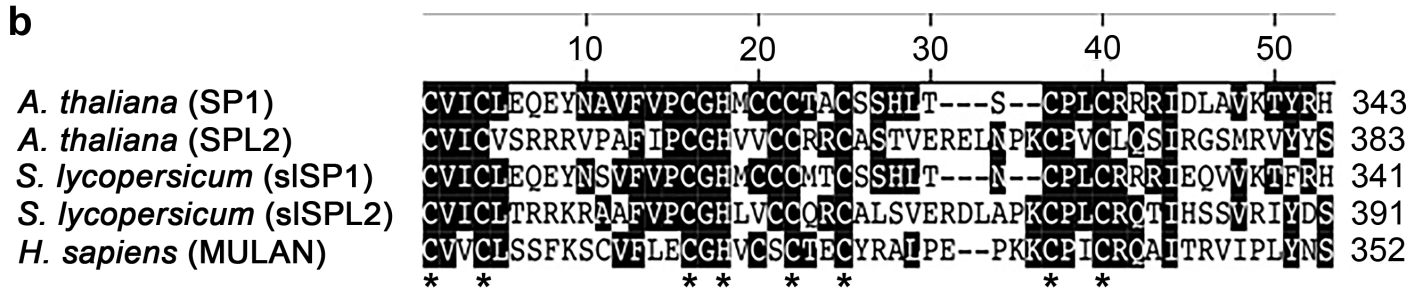
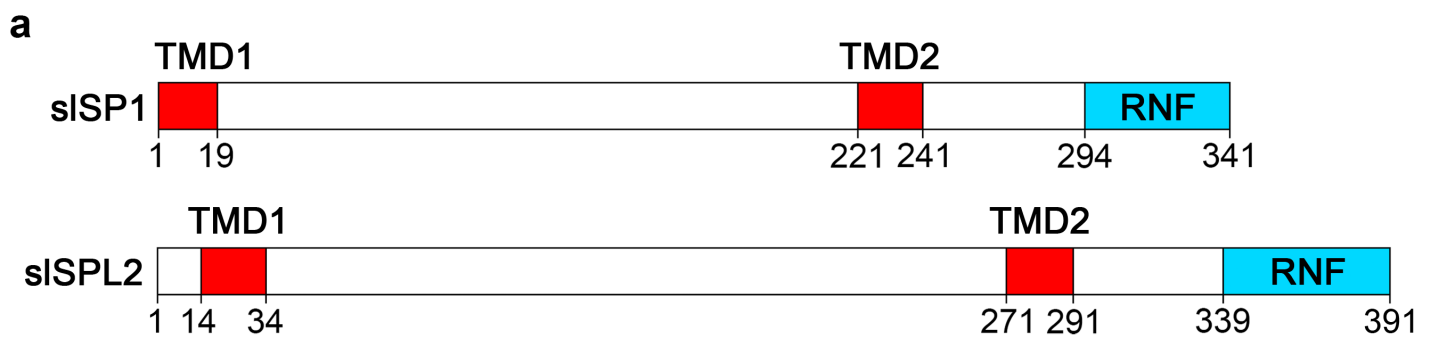
791

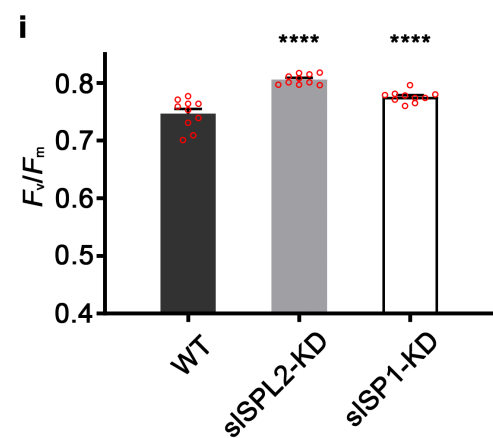
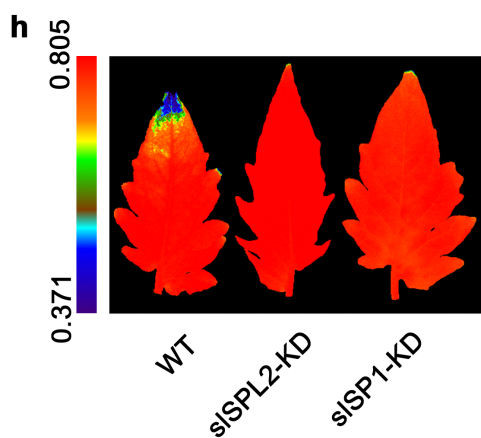
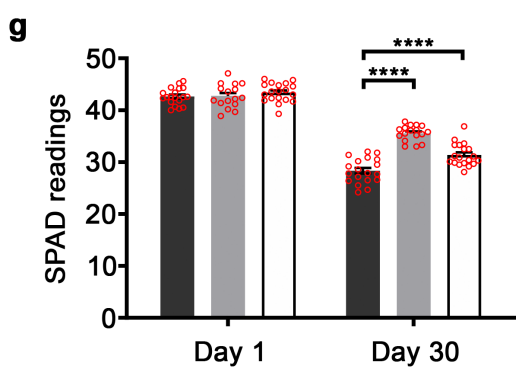
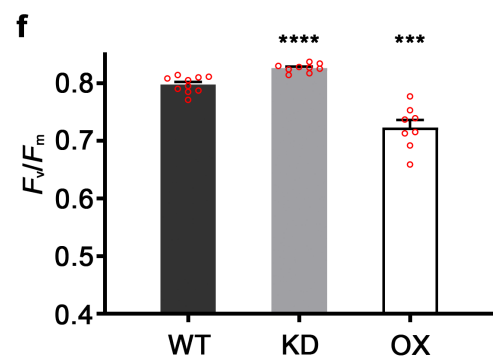
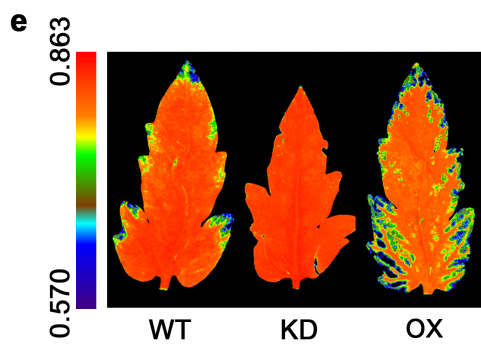
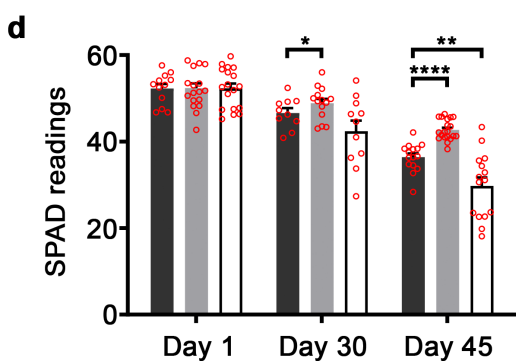
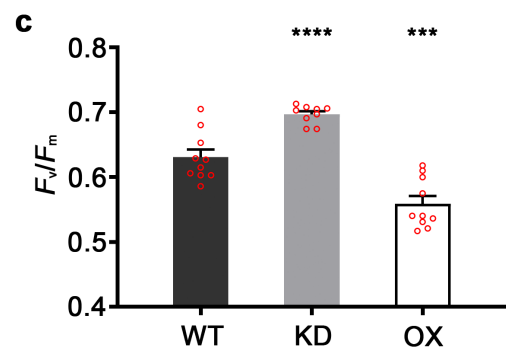
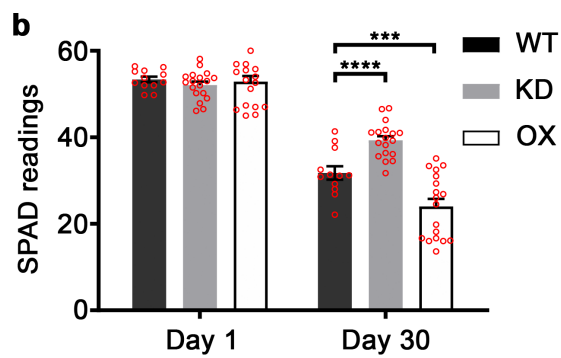
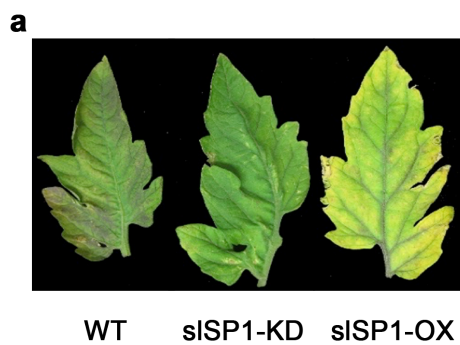
792 **Fig. 6 | Analysis of the role of slSP1 in regulating the plastid proteome during leaf**
793 **senescence and fruit ripening.** **a,b**, Immunoblot analysis of total protein extracts from

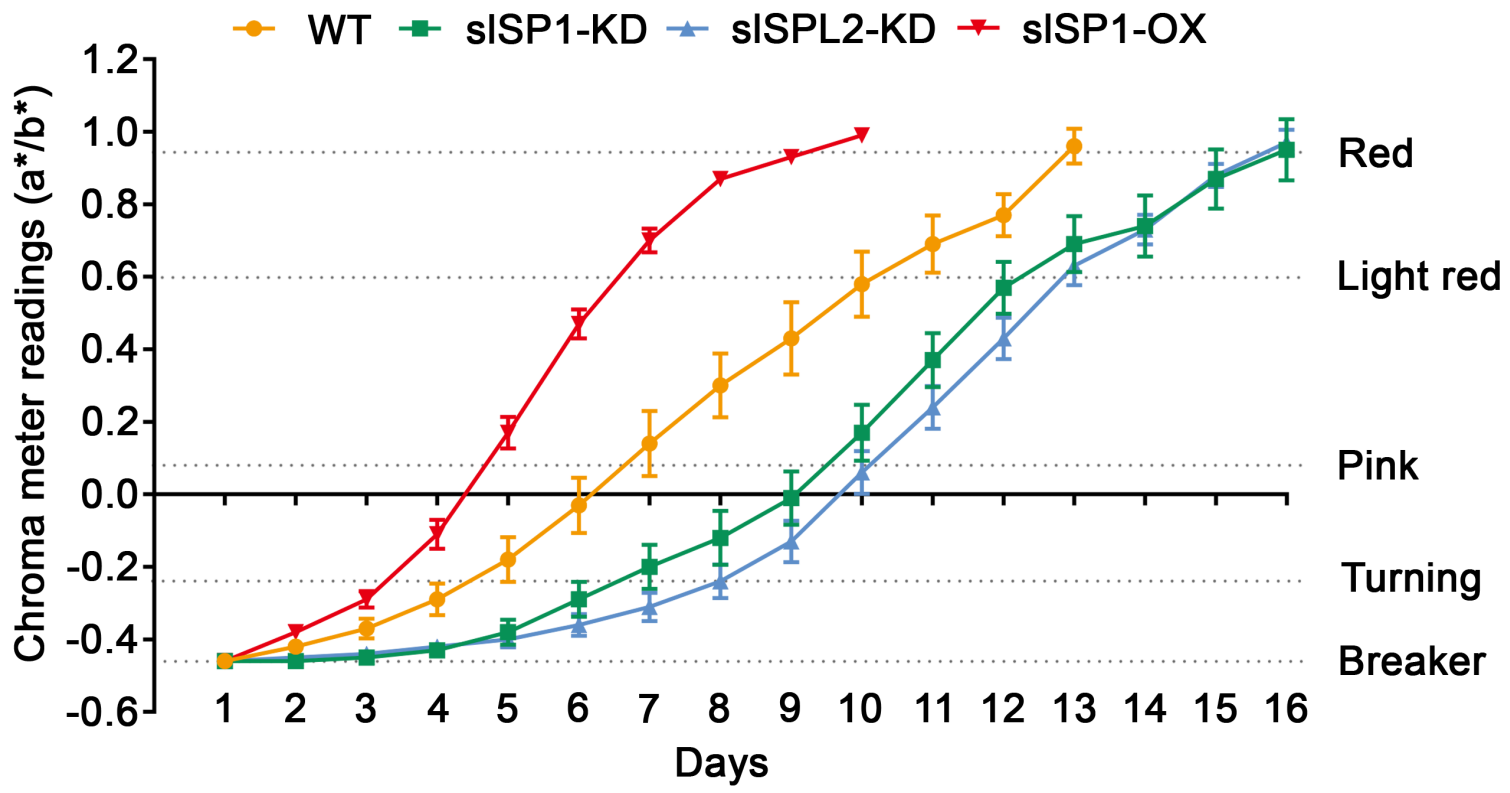
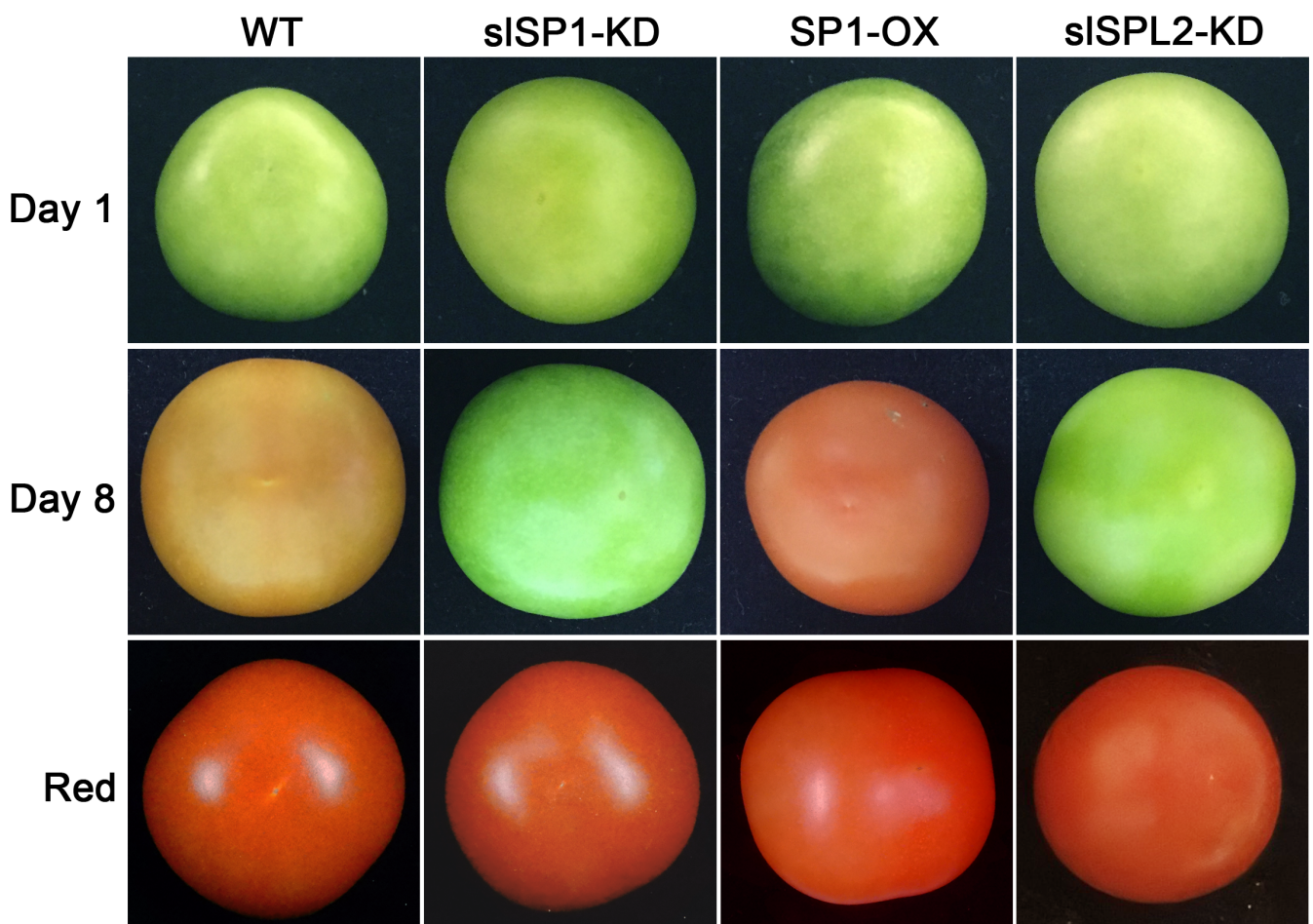
794 leaves of 2-week-old plants of the indicated genotypes, using Toc75, Tic40, and histone H3
795 (as a loading control) antibodies ($n = 10-15$ experiments; *** $p = 0.0003$ [Toc75, KD] and
796 **** $p = 0.0001$ [Toc75, OX], compared with WT). **c,d**, Immunoblot analysis of total protein
797 extracts from leaves of 2-month-old plants that had been induced to senesce by dark
798 treatment, using Toc75, Tic40, PsbO (OE33), and H3 antibodies ($n = 3-8$ experiments; **** p
799 $= 0.0001$ [Toc75, KD], **** $p = 0.0001$ [Toc75, OX], * $p = 0.0156$ [PsbO, KD], and * $p =$
800 0.0398 [PsbO, OX], compared with WT). **e,f**, Immunoblot analysis of total protein extracts
801 from Day 8 post-breaker stage fruit, using Toc75, Tic40, PsaD, PGL35 and H3 antibodies (n
802 $= 3-4$ experiments; ** $p = 0.0073$ [Toc75, KD], * $p = 0.0206$ [Toc75, OX], * $p = 0.0117$ [PsaD,
803 KD], ** $p = 0.0080$ [PsaD, OX], and ** $p = 0.0068$ [PGL35, KD], compared with WT). In
804 each case, the protein bands were visualized by chemiluminescence imaging, and then

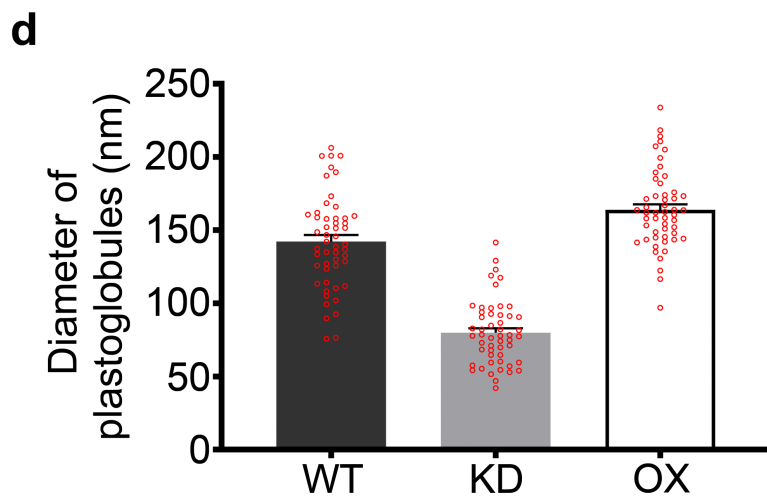
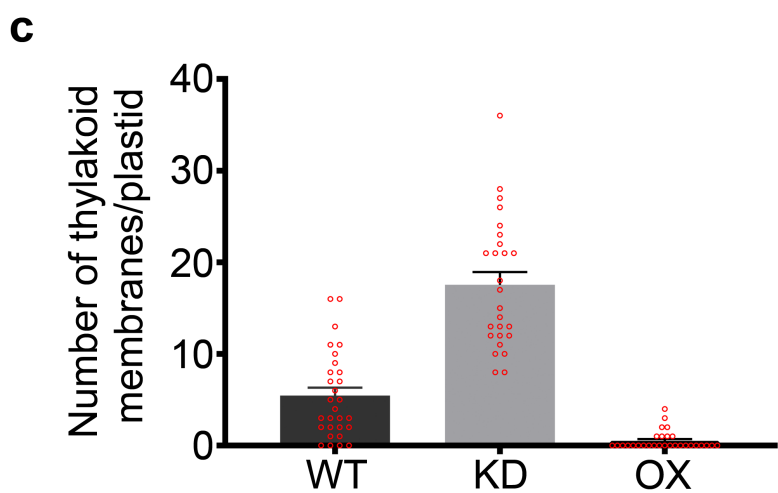
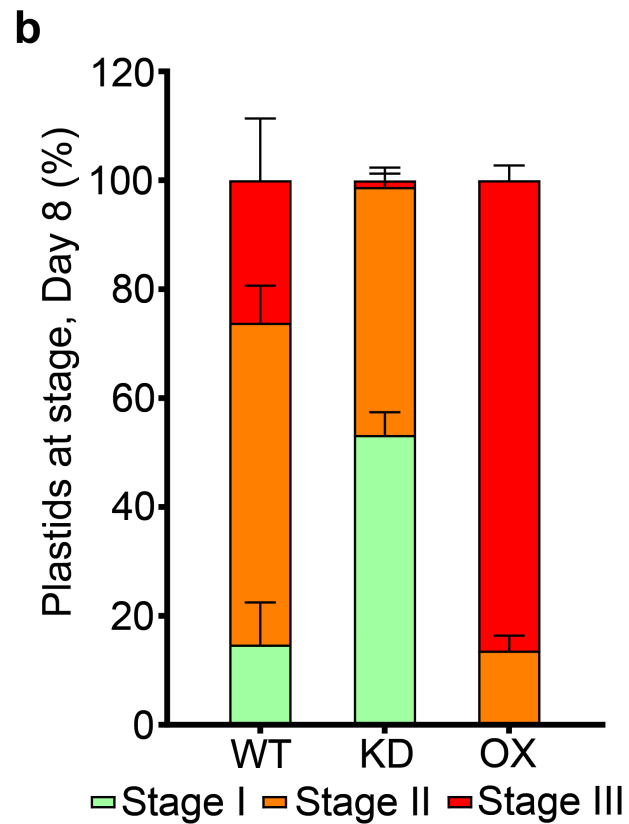
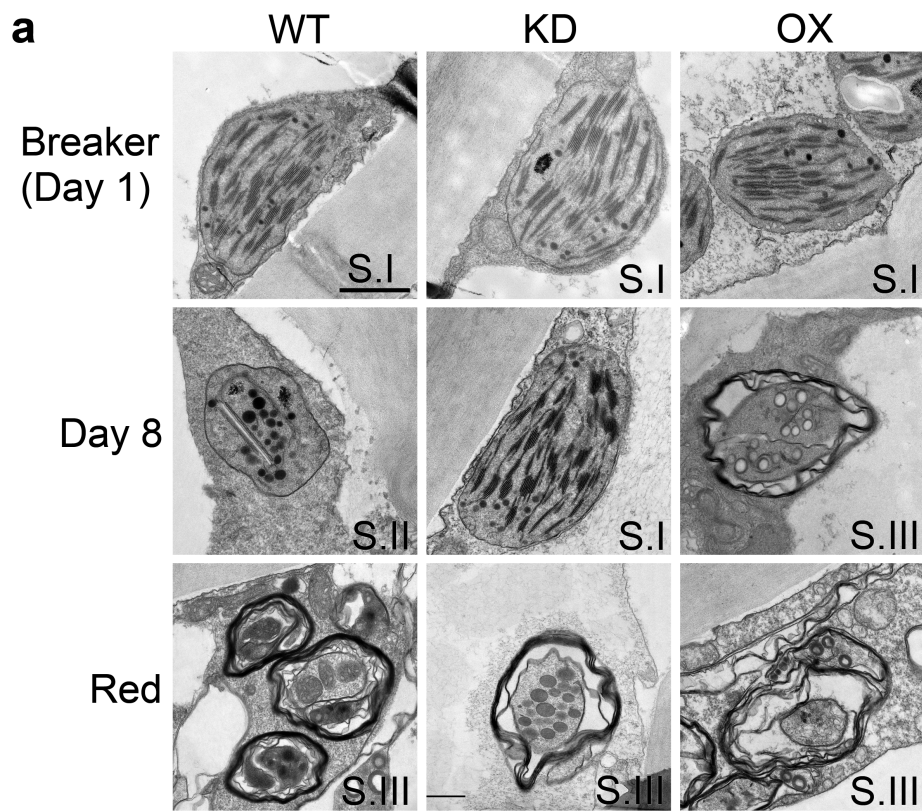
805 quantified by using Aida software. The data obtained for proteins of interest were normalized
806 relative to corresponding H3 data. All values are expressed relative to the corresponding
807 value for WT, which in each case is set to 1. Values are means \pm SEM of at least three
808 replicates. The p values were derived from an unpaired two-tailed Student's t -test; WT was
809 used as the reference group for the statistical analysis. Positions of molecular weight markers
810 are shown to the right of the images (a,c,e).

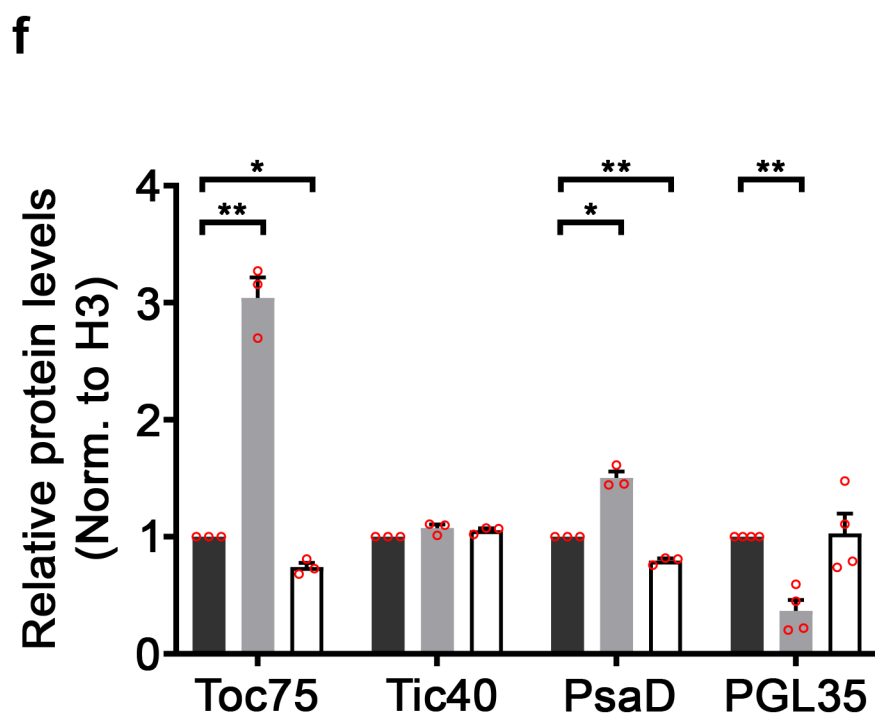
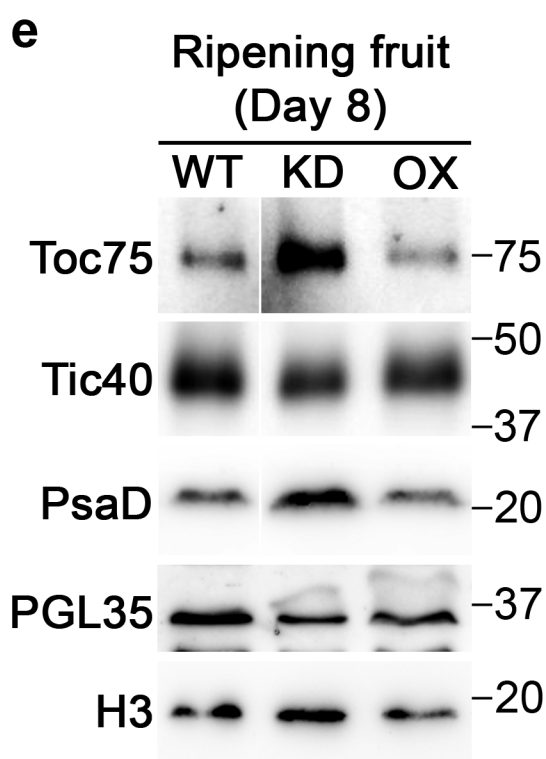
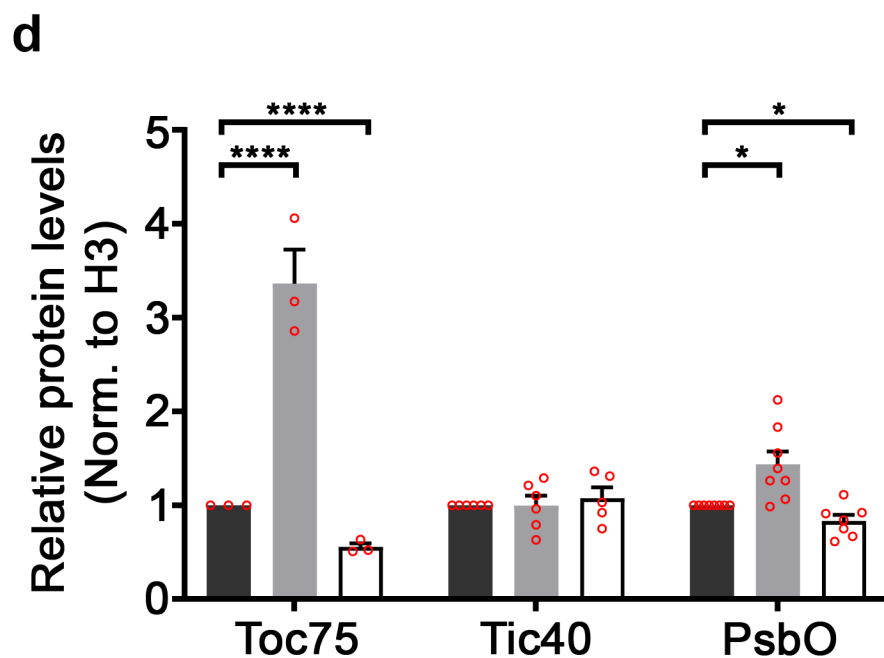
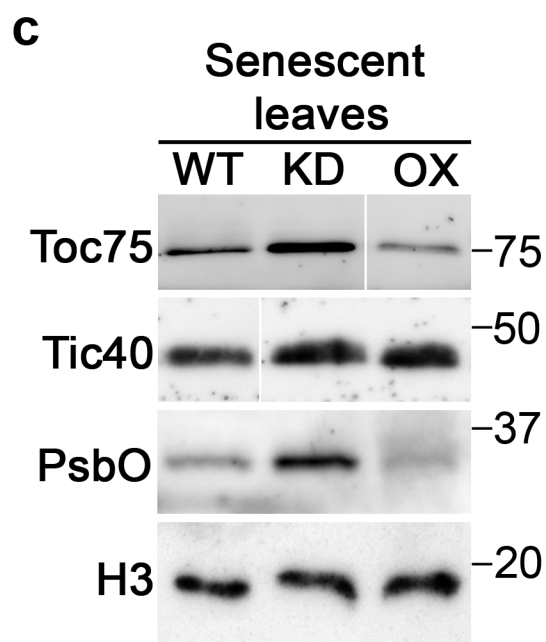
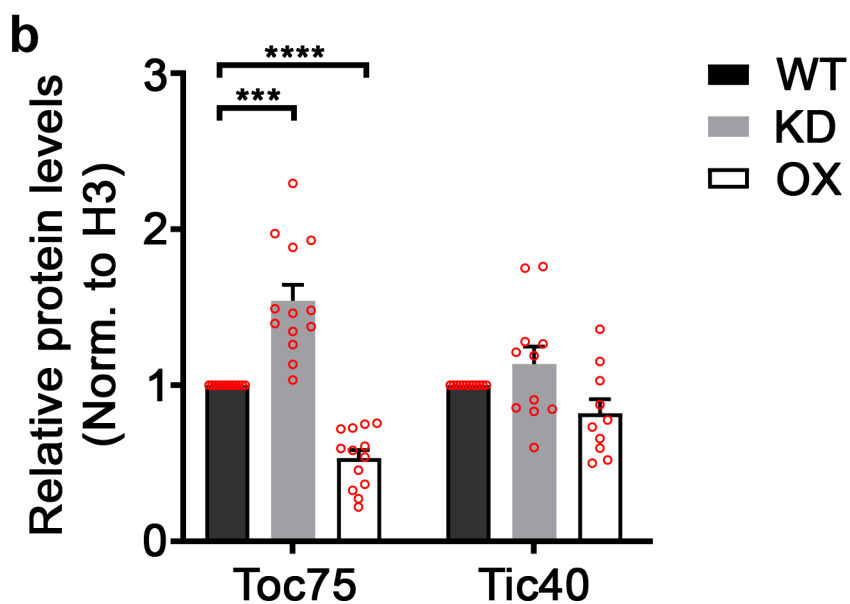
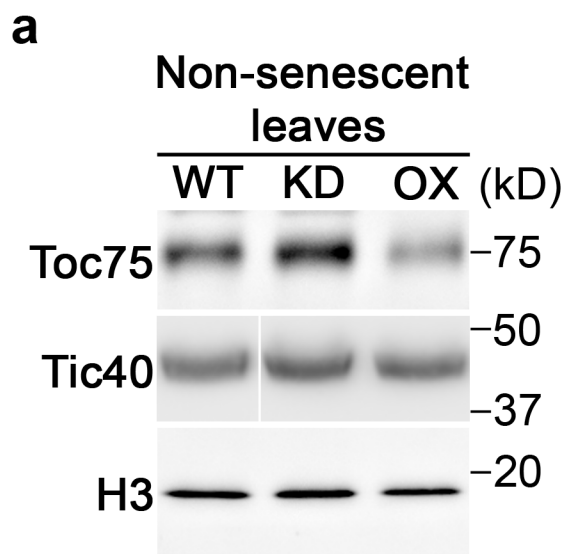
811





a**b**





812 **Methods**

813 **Plant growth conditions**

814 Tomato (*Solanum lycopersicum* cv. Ailsa Craig) was grown in Levington M2 modular
815 compost mixed with a slow release fertilizer, and were kept adequately watered. The
816 greenhouse was kept at a constant temperature of 25°C, with a light cycle of 16 hours of light
817 followed by 8 hours of darkness.

818 Dark treatments for the induction of leaf senescence were conducted using the following
819 method that was previously described for use with *Arabidopsis*¹⁹. Developmentally-
820 equivalent leaves of approximately 2-month-old plants were wrapped in aluminium foil
821 whilst still attached to the plants, and then left under standard growth conditions for 16 to 30
822 days. For age-related leaf senescence analysis, leaves similar to those above were selected
823 and marked (with paper tags), and then left uncovered as the plants were grown on under
824 standard conditions for up to 45 days. In both cases, the degree of senescence was analysed
825 by making measurements of chlorophyll content and photosynthetic efficiency at the end (and
826 beginning) of the experiment.

827 **Chlorophyll measurements**

828 Leaf chlorophyll contents were measured using a SPAD-502 meter (Konica Minolta)
829 following the instructions from the manufacturer⁵².

830 **Quantification of photosynthetic efficiency**

831 Chlorophyll fluorescence imaging was performed on freshly detached leaves using a CF
832 Imager (Technologica Limited). Plants were dark-adapted for 30 minutes immediately before
833 the leaves were detached for each measurement. The data were used to calculate the F_v/F_m
834 ratio, to provide an estimation of the maximum photochemical efficiency of photosystem II in
835 dark-adapted material⁵³. At least 3 leaves (from 3 plants) were analysed per genotype in each
836 experiment.

837 **Identification and *in silico* analysis of tomato SP1 homologues**

838 Tomato SP1 homologue sequences were obtained by BLAST searches of the Phytozome,
839 Ensembl Plants, and National Center for Biotechnology Information (NCBI) databases using
840 the Arabidopsis SP1 amino acid sequence as a query⁵⁴. Alignments were performed using

841 Clustal W⁵⁵, and RNF domains were predicted based on the alignment results.
842 Transmembrane domains were predicted based on the alignment results and by using
843 Aramemnon (TmMultiCon)⁵⁶. Sequence files were managed using DNASTar Lasergene v7.2.

844 **Constructs and tomato transformation**

845 All primers used are listed in Supplementary Table 1. To generate the *slSP1*-OX construct,
846 the complete CDS of *slSP1* (Solyc06g084360) was amplified from tomato cDNA and
847 inserted using Gateway cloning into the pDONR201 entry vector. The *slSP1*-KD and *slSPL2*-
848 KD constructs encoded artificial microRNA (amiRNA) sequences that were designed to
849 specifically target the respective gene^{57,58}. The amiRNA target sequences are listed in
850 Supplementary Table 1b. The amiRNAs were designed using the WMD3 Web MicroRNA
851 Designer⁵⁹, and carefully selected to ensure gene silencing efficiency and specificity. They
852 were amplified from tomato cDNA using the primers listed in Supplementary Table 1c. The
853 resulting sequences were cloned into the pRS300 vector⁵⁹ to make the amiRNA precursors,
854 and then amplified and inserted using Gateway cloning into the pDONR201 entry vector.

855 The *slSP1* CDS and amiRNA precursor sequences (for both *slSP1* and *slSPL2*) were
856 subsequently cloned into the binary vector pK7WG2D, which contains the neomycin
857 phosphotransferase II (*nptII*) gene conferring kanamycin resistance and a green fluorescent
858 protein (GFP) marker to aid callus selection⁶⁰, using a Gateway Clonase II kit (Invitrogen).
859 This generated the pK7WG2D-*slSP1* (*slSP1*-OX), pK7WG2D-amiR*slSP1* (*slSP1*-KD), and
860 pK7WG2D-amiR*slSPL2* (*slSPL2*-KD) vectors. The resulting plasmids were freeze-thaw
861 transformed into the *Agrobacterium tumefaciens* strain GV3101 (pMP90RK)⁶¹. Plasmids
862 were isolated from *Agrobacterium* and verified by restriction digestion prior to use in tomato
863 transformation experiments.

864 Tomato plant transformation was conducted by following a published protocol with minor
865 modifications⁶². Before *Agrobacterium* infection, tomato cotyledon leaf segments were
866 prepared by removing the apical and basal extremities, placed on solid KCMS medium (4.4
867 g/L Murashige-Skoog [MS] salts with vitamins, 20 g/L sucrose, 200 mg/L KH₂PO₄, 0.9 mg/L
868 thiamine, 100 µM acetosyringone, 8 g/L agar, pH 5.7) and incubated at 25°C for 24 hours.
869 Leaf segments were co-cultivated with the *Agrobacterium* suspension (diluted in liquid
870 KCMS medium [KCMS without agar] to a final optical density of 0.05) for 30 minutes with
871 shaking. The segments were then dried on sterile filter paper, placed on solid KCMS
872 medium, and incubated for 2 days at 25°C. The inoculated segments were cultured on 2Z

873 medium (4.4 g/L MS salts with vitamins, 30 g/L sucrose, 2 mg/L zeatin riboside, 150 mg/L
874 timentin, 75 mg/L kanamycin, 8 g/L agar, pH 5.8) for shoot regeneration. The medium was
875 changed every 10 to 14 days. Newly formed shoots were cut from the calli and placed in
876 rooting medium (4.4 g/L MS basal salts without vitamins, 30 g/L sucrose, 1 mg/L indole-3-
877 acetic acid [IAA], 150 mg/L timentin, 30 mg/L kanamycin, 6 g/L agar, pH 5.8). The ploidy
878 number of the transformants was checked by counting the number of chloroplasts in guard
879 cells, and only diploid plants were selected for further analysis⁶³. The most suitable lines
880 were grown to maturity, and T1 seeds were harvested. Transformed plants were analysed by
881 quantitative genomic PCR of the *nptII* selectable marker gene in the T1 generation, to
882 determine copy number and identify homozygous lines, and only homozygous lines with a
883 single T-DNA insertion were selected for further analysis. The overexpression or silencing of
884 *sLSP1* and *sLSP2* in the T0 and T1 generations was assessed by RT-PCR, relative to
885 expression in wild-type plants regenerated from tissue culture in parallel, and the data were
886 normalized to *sLACTIN* (Solyc03g078400).

887 **Subcellular localization analysis**

888 To produce the YFP fusion constructs for subcellular localization analysis, CDSs of *sLSP1*
889 and *sLSP2* without the stop codon were amplified from tomato cDNA by PCR using primers
890 listed in Supplementary Table 1a. Amplicons were subsequently cloned, via pDONR201, into
891 the plant expression vector p2GWY7 to provide a C-terminal YFP tag⁶⁴. The Gateway system
892 (Invitrogen) was used for the cloning, and both constructs were verified by DNA sequencing.

893 Tomato mesophyll protoplast isolation and transient assays were both carried out using an
894 established method, with modifications^{19,65}. In brief, the first pair of leaves from
895 approximately 2-week-old plants were collected, and the abaxial epidermis was peeled off
896 using Magic tape (3M) and discarded. The peeled leaves were incubated in enzyme solution
897 (1% cellulase 'Onozuka' R10 [Yakult, Tokyo, Japan], 0.25% macerozyme 'Onozuka' R10
898 [Yakult], 0.4 M mannitol, 10 mM CaCl₂, 20 mM KCl, 0.1% bovine serum albumin [BSA],
899 20 mM 2-morpholinoethanesulfonic acid [MES], pH 5.7) for 2 hours with gentle shaking.
900 The released protoplasts were collected by centrifugation at 100 × g for 3 min, washed twice
901 with 25 mL pre-chilled W5 solution (154 mM NaCl, 125 mM CaCl₂, 5 mM KCl, 5 mM
902 glucose, 2 mM MES, pH 5.7) and incubated on ice for 30 min. The protoplasts were then
903 counted, collected by centrifugation at 100 × g for 3 min, and resuspended in MMg solution
904 (0.4 M mannitol, 15 mM MgCl₂, 4 mM MES, pH 5.7) to a final concentration of 1 × 10⁶

905 cells/mL. Approximately 0.1 mL protoplast suspension was mixed with 5 µg plasmid DNA at
906 room temperature. An equal volume of a freshly-prepared polyethylene glycol (PEG) solution
907 (40% [w/v] PEG-4000 [Fluka], 0.1 M CaCl₂, 0.2 M mannitol) was added, gently mixed, and
908 incubated at room temperature for 5 min. After incubation, the solution was gently mixed
909 with 1.5 mL W5 solution, and the protoplasts were pelleted by centrifugation at 100 × *g* for 2
910 min. This protoplast W5 washing step was repeated twice more, and the protoplasts were
911 finally incubated in 0.5 mL W5 in 24-well plates at room temperature for 15-18 hours in the
912 dark.

913 Fluorescence images were captured using a Nikon Eclipse TE-2000E inverted microscope
914 and NIS Elements v4.00 software (Nikon)^{19,66}. Fluorescence signals were analysed with
915 filters for YFP (exciter HQ500/20x, emitter HQ535/30m) and chlorophyll autofluorescence
916 (exciter D480/30x, emitter D660/50m) (Chroma Technology). All experiments were
917 conducted at least twice with the same results, and typical images are shown.

918 **Analysis of tomato plant DNA and RNA**

919 Extraction of tomato DNA and RNA, and quantitative RT-PCR (qRT-PCR), were performed
920 using the following established methods⁶⁶. In brief, DNA and RNA extractions were done
921 using a DNeasy Plant Mini Kit (Qiagen) and a Spectrum Plant Total RNA Kit (Sigma-
922 Aldrich), respectively. Reverse transcription was performed by using SuperScript IV Reverse
923 Transcriptase (Invitrogen). For qRT-PCR, a PowerUp SYBR Green Master Mix Kit (Applied
924 Biosystems) and a StepOnePlus Real-Time PCR System (Applied Biosystems) were
925 employed. The primers used for PCR amplification are shown in Supplementary Table 1d.
926 Gene expression data were normalized using data for *slACTIN*.

927 For qRT-PCR analysis of different tissues, root, stem and leaf tissues from 4-week-old
928 tomato plants were used; and, petal and sepal flower parts from 2-month-old tomato plants
929 were used. For qRT-PCR analysis of fruit, samples were collected from the fruit mesocarp of
930 developing (0.5 cm fruit diameter), pre-mature green (dark green), mature green (light green),
931 breaker, pink and red fruit stages, with later stages being differentiated using a Chroma Meter
932 (Konica Minolta)³³.

933 **Fruit ripening analysis**

934 The ripening analysis was carried out using fruits selected at the onset of breaker stage. Fruits
935 at breaker stage were harvested and placed in a Percival growth chamber without lights at a

936 constant temperature of 25°C with 60% humidity. Then, fruit colour values were recorded on
937 a daily basis all the way through to the mature red stage. Fruit colour was measured by
938 reflectance using a Chroma Meter Model CR 400 (Konica Minolta), which records a*/b*
939 values, an established indicator of colour development and maturation in tomato^{67,68}. The a*
940 value represents colours from green to red (it denotes greenness when negative, and redness
941 when positive), whereas the b* value represents colours from blue to yellow (it denotes
942 blueness when negative, and yellowness when positive). Konica Minolta a*/b* values of
943 tomatoes correspond to United States Department of Agriculture (USDA) colour stages, as
944 follows³³: breaker, -0.47; turning, -0.27; pink, 0.08; light red, 0.60; red, 0.95. Each fruit was
945 measured at four different positions at the bottom of the fruit, and a mean value was
946 calculated and used.

947 **Fruit size**

948 The maximal lateral diameter of tomato fruit was measured using a Digital Caliper 150 mm
949 (Fisher Scientific Traceable) when the fruit reached breaker stage. As noted above, the fruit
950 were then detached from the plant and incubated at 25°C in the dark for use in ripening
951 analysis.

952 **Fruit firmness**

953 Fruit firmness was measured using a Durofel XF basic durometer (Agrosta Sarl). An average
954 value derived from four readings recorded at four different points on the circumference of
955 each fruit was calculated and used. The firmness measurement scale was 0-100 in durometer
956 units. Values higher than 70 units indicated hard tomatoes, and those less than 60 units
957 indicated soft tomatoes⁶⁹.

958 **Transmission electron microscopy**

959 Tomatoes were sampled near the base of the fruit using a scalpel, and the pieces were
960 transferred to a Leica AMW sample basket for microwave processing (microwave-assisted
961 chemical fixation was performed to increase speed of fixation and reduce plasmolysis). Fresh
962 fixative was used for each batch, and consisted of: 2.5% (v/v) glutaraldehyde plus 4%
963 paraformaldehyde (w/v) in 0.1 M sodium cacodylate buffer, pH 6.9. After fixation, samples
964 were incubated at room temperature for 5 hours and then transferred to 4°C for 2 days.
965 Subsequent processing steps were performed with microwave assistance. Samples were
966 transferred to AMW baskets and then processed in the Leica AMW using Program 1 (buffer

967 wash; staining with 2% osmium tetroxide (w/v) plus 1.5% potassium ferricyanide (w/v) in
968 0.1M sodium cacodylate buffer, pH 6.9; water washing; en-bloc staining with 2% uranyl
969 acetate (w/v); water washing; first part of ethanol dehydration) and, following a reagent
970 change, with Program 2 (ethanol and acetone dehydration; then infiltration with TAAB Hard
971 Plus epoxy resin). Following completion of Program 2, the baskets were disassembled and
972 samples were submerged in fresh 100% TAAB Hard Plus epoxy resin and placed on a rotator
973 for 24 hours. Samples were then embedded in fresh resin in flat dish embedding moulds and
974 polymerised at 65°C for 48 hours. Semithin (500 nm) and ultrathin (90 nm) sections were
975 taken from each block using a Leica UC7 ultramicrotome equipped with a Dیتome diamond
976 knife. Semithin sections were transferred to glass slides and stained with Toluidine blue for
977 preliminary inspection. Ultrathin sections were transferred to formvar coated 50 mesh copper
978 grids or 2 mm × 1 mm slot grids and post-stained for 5 minutes with lead citrate. Grids were
979 imaged at 120 kV in a FEI Tecnai 12 TEM using a Gatan OneView camera. Quantitative data
980 were derived from at least 30 different plastids per genotype, or more than 50 different
981 plastoglobules per genotype, and are representative of three individuals per genotype.

982 **Profiling of tomato fruit metabolites**

983 Sample preparation and metabolite profiling of tomato fruit tissues was carried out using
984 established methods. Tomatoes were sampled exactly as described above for TEM analysis,
985 taking equivalent tissue. The samples were immediately covered with aluminium foil and
986 subjected to freeze-drying in an Alpha 2-4 LD (Martin Christ) for at least two days. Then the
987 freeze-dried fruit pieces were ground into a fine powder in liquid nitrogen, and were stored at
988 -80°C or used in following HPLC, IC-MS and GC-MS analyses.

989 For HPLC analysis of pigments, approximately 15 mg fruit tissue powder was mixed with 1
990 mL hexane/acetone/methanol 2:1:1 as an extraction solvent and 25 µL of a 10% (w/v)
991 solution of canthaxanthin (Sigma) in chloroform as an internal control. The mixture was
992 vortexed for 10 seconds and lysed using 4 mm glass beads for 1 minute at 30 Hz in a
993 TissueLyser II (Qiagen) homogenizer. After adding 100 µL milli-Q water and mixing for 1
994 minute in the TissueLyser, samples were centrifuged for 3 minutes at 500 × g and 4°C. The
995 organic phase was evaporated using a SpeedVac system, and the extracted pigments were
996 resuspended in 200 µL acetone by using an ultrasound bath (Labolan). Separation and
997 detection of carotenoids was next performed using an Agilent 1200 series HPLC system
998 (Agilent Technologies)¹⁷. Eluting chlorophylls and carotenoids were monitored using a

999 photodiode array detector, whereas tocopherols were identified using a fluorescence detector.
1000 Peak areas of chlorophylls (650 nm), coloured carotenoids (470 nm for lycopene, β -carotene,
1001 lutein and canthaxanthin), phytoene (280 nm), and tocopherols (330 nm) were determined
1002 using Agilent ChemStation HPLC 2D 32 bit, version G2175BA, software. Quantification was
1003 performed by comparison with commercial standards (Sigma).

1004 For IC-MS analysis, approximately 50 mg fruit powder was further homogenized in a
1005 Precellys Evolution homogenizer (Bertin Instrument) with 500 μ L 100% methanol solvent (a
1006 100 mg/mL final ratio) and ceramic beads; homogenization was undertaken in two steps,
1007 each at 100% power for 10 seconds with a 20 second interval between steps to prevent
1008 sample heating. Samples were filtered through Ultra Centrifugal Filters (10 kD cut-off;
1009 Amicon) to remove proteins, and processed using a Dionex Ultimate 3000 UHPLC system
1010 (Dionex) coupled to a Q-Exactive HF hybrid quadrupole-Orbitrap mass spectrometer
1011 (Thermo Scientific)⁷⁰. The data were analysed using Progenesis QI version 2.0 for small
1012 molecules (Waters).

1013 For GC-MS, metabolites were extracted by mixing approximately 10 mg fruit powder with
1014 400 μ L 100% methanol solvent and 60 μ L of a 0.1 mg/mL solution of ribitol (Sigma-Aldrich)
1015 as an internal standard. Extraction was done by brief vortexing and then shaking for 15
1016 minutes at 70°C. Samples were centrifuged for 10 minutes at 20,000 $\times g$, and then the
1017 supernatants were further extracted by mixing with 250 μ L chloroform and 500 μ L water
1018 through vortexing. After centrifugation for 15 minutes at 2000 $\times g$, 100 μ L polar phase was
1019 analysed using an Intuvo 9000 GC system (Agilent Technologies) coupled to a 5977 Series
1020 MSD detector (Agilent Technologies)⁷¹. The data were analysed using Agilent MassHunter
1021 Workstation Software, Quantitative Analysis, version B.08.00 for GC-MS.

1022 In Figure 5, lycopene, phytoene, lutein, chlorophylls, tocopherols were detected by HPLC;
1023 neoxanthin, caffeic acid, galacturonic acid, arginine, methionine, glycerol were detected by
1024 IC-MS; glutamic acid, alanine, glycine, serine and lysine were detected by GC-MS.

1025 **Tomato protein extraction**

1026 Tomato leaf protein extraction was conducted by following a procedure similar to that
1027 described previously for *Arabidopsis*⁷². Approximately 20 mg leaf tissue was used for each
1028 sample, and only leaf lamina tissue was collected to avoid the thick midvein.

1029 Tomato fruit protein extraction was performed using a published method⁷³. Tomato fruit
1030 tissue was ground in liquid N₂ to a fine powder using a TissueLyser (Qiagen) at 20 Hz for 1
1031 minute. Ground tissue samples (1 g) were each suspended in 3 mL extraction buffer (500 mM
1032 Tris-HCl, 50 mM ethylenediaminetetraacetic acid [EDTA], 700 mM sucrose, 100 mM KCl,
1033 pH 8.0; 2% (v/v) β-mercaptoethanol and 1 mM phenylmethylsulfonyl fluoride were added
1034 just before use) by vortexing, and incubated on ice with shaking for 10 minutes. An equal
1035 volume of Tris-buffered phenol was added to each sample, and samples were incubated with
1036 shaking (180 rpm) at room temperature for 10 minutes. After centrifugation at 5500 × g and
1037 4°C for 10 minutes (all centrifugation steps below were similar), the upper phenolic phase
1038 was recovered in each case, and an additional 3 mL extraction buffer was added and mixed
1039 thoroughly before further centrifugation. The phenolic phase was again recovered to a new
1040 tube, and then four volumes of precipitation solution (0.1 M ammonium acetate in cold
1041 methanol) was added per sample, with mixing by inverting the tubes. Samples were
1042 incubated at -20°C for 4 hours or overnight, and then proteins were pelleted by centrifugation.
1043 Pellets were washed three times with ice-cold precipitation solution, and finally with ice-cold
1044 acetone; after each washing step, the samples were centrifuged. The final pellet was dried
1045 under vacuum for 1 hour, and then resuspended in 2 × protein loading buffer (4% [w/v]
1046 sodium dodecyl sulphate [SDS], 20% [v/v] glycerol, 120 mM Tris-HCl, pH 6.8, 50 mM
1047 dithiothreitol, 0.02% [w/v] bromophenol blue).

1048 **SDS-PAGE, immunoblotting and quantification**

1049 For SDS-PAGE, immunoblotting and quantification thereof, procedures were as previously
1050 described^{74,75}. Total protein samples of 10 to 20 µg, prepared from tomato leaf or fruit, were
1051 typically analysed. Primary antibodies were: anti-atToc75-III (Translocon at the outer
1052 envelope membrane of chloroplasts, 75 kD) antibody⁷⁶, anti-atTic40 (Translocon at the inner
1053 envelope membrane of chloroplasts, 40 kD) antibody⁶⁶, anti-PsbO/OE33 (Photosystem II
1054 subunit O / Oxygen evolving complex, 33 kD) antibody^{19,77}, anti-PsaD (Photosystem I
1055 subunit D) antibody⁷⁸, anti-PGL35 (Plastoglobulin 35) antibody (Agrisera)⁷⁹, and anti-H3
1056 histone antibody (Abcam)⁶⁶. Secondary antibody was anti-rabbit immunoglobulin G (IgG)
1057 conjugated with horseradish peroxidase (Santa Cruz Biotechnology). Chemiluminescence
1058 employed an EZ-ECL Chemiluminescence Detection Kit (Geneflow) and an ImageQuant
1059 LAS-4000 imager (GE Healthcare Life Sciences). Bands intensities were quantified in silico
1060 using Aida Image Analyzer v4.27 Software (Raytest). Quantification data were obtained from

1061 the results of at least three experiments all showing a similar trend, and typical images are
1062 shown.

1063 **Statistical analysis**

1064 Statistical calculations (mean, standard error of the mean [SEM], and *t*-test) were performed
1065 by using GraphPad Prism v8.3.0 software. The statistical significance of differences between
1066 two experimental groups was assessed by using an unpaired two-tailed Student's *t*-test.
1067 Differences between two datasets were considered significant at $p < 0.05$. The wild type was
1068 used as the reference group for all statistical analyses.

1069 **Data availability**

1070 All data generated or analysed during this study are included in this published article or its
1071 supplementary information.

1072 All unique materials are readily available from the authors upon request.

1073

1074

Extended Data Figure Legends

Extended Data Fig. 1 | Expression profiles of the *sISP1* and *sSPL2* genes. The expression profiles shown are based on Affymetrix GeneChip data and were generated using the Development (**a**) and Anatomy (**b**) functions of Genevestigator⁸⁰. Data from ATH arrays are shown in scatter-plot diagrams. In **a**, the x-axis represents the following developmental stages, from left to right: young seedling, developed seedling, flower, green fruit, ripening fruit, and mature fruit. Values are means \pm SEM, and for each data point the number of samples is indicated. Medium expression levels are defined as the interquartile range (IQR; light grey boxes); values below the IQR are defined as low expression (white boxes), and values above the IQR as high expression (HIGH; dark grey boxes). The presented data provide a complement to the data in Fig. 1d, and confirm that *sSPL2* is generally more weakly expressed than *sISP1*.

Extended Data Fig. 2 | Assessment of the extent of knockdown or overexpression of the *sISP1* and *sSPL2* genes in the transgenic tomato plants. Total leaf RNA was extracted from 2-week-old tomato plants of the indicated genotypes; three independent T1 generation transformants (#1-3) were analysed for each construct. Quantitative RT-PCR analysis of *sISP1* and *sSPL2* expression was performed on the corresponding transgenic lines, in comparison with wild-type controls, as indicated. Relative gene expression levels were calculated by normalization using the reference gene, *sACTIN*. All values are expressed relative to the corresponding value for wild type, which in each case is set to 1. Values are means \pm SEM ($n = 3$ [WT-1, *sSPL2*-KD #2 and #3], 4 [*sISP1*-KD #3], or 5 [all other genotypes] technical replicates).

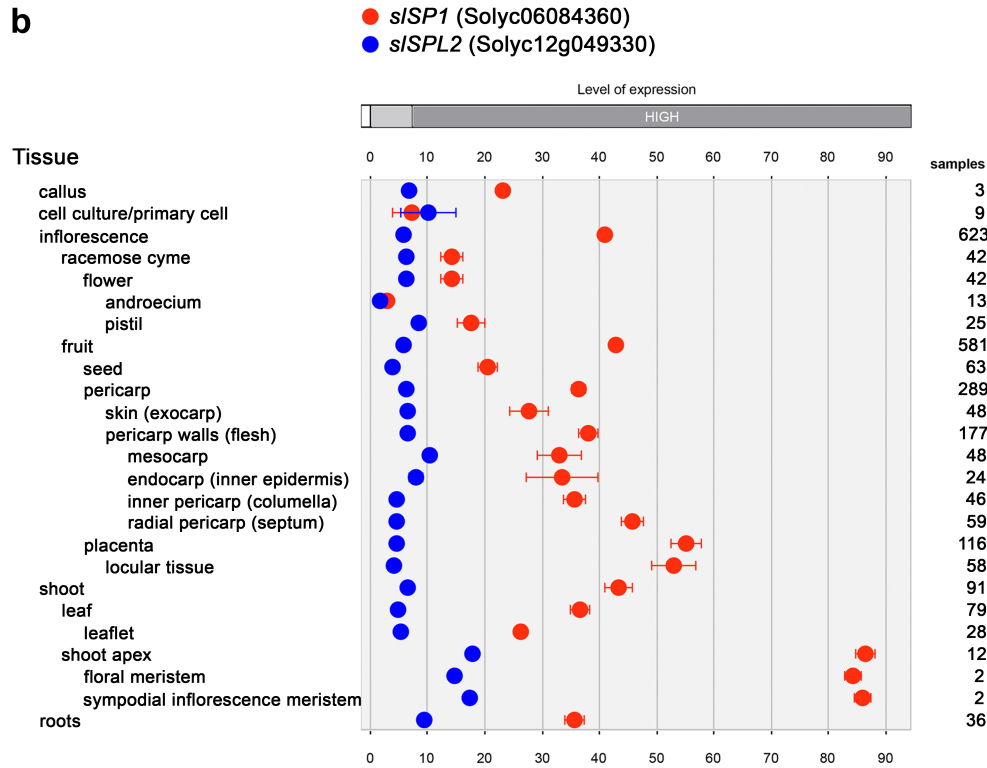
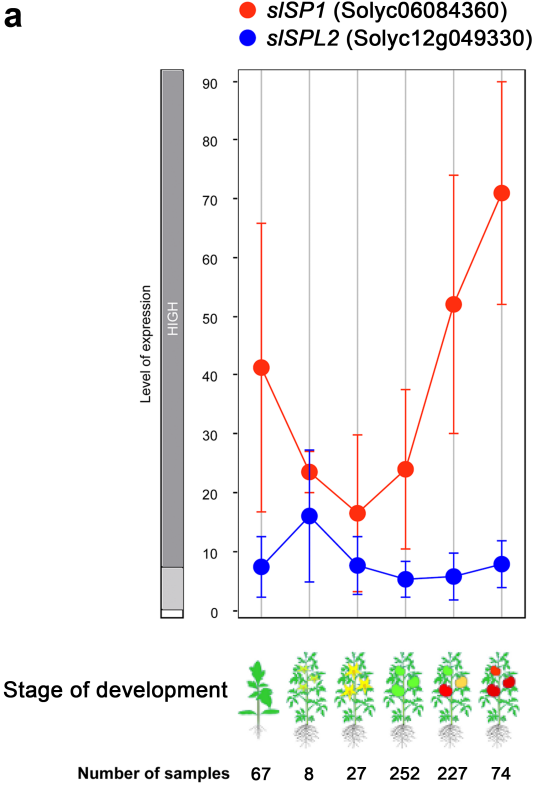
Extended Data Fig. 3 | Determination of tomato fruit sizes. Measurement of the maximal equatorial diameter of Day 8 breaker-stage tomato fruit, from T2 generation transgenic plants, was performed using a calliper. The fruits were then detached from the plants and incubated at 25°C in the dark for the ripening analysis presented in Figure 3. Values are means \pm SEM ($n = 26-27$ fruits per genotype). The data demonstrate that fruit size in the *sISP1*-KD, *sISP1*-OX and *sSPL2*-KD transgenic lines at breaker stage was not significantly different from that in the wild type, as revealed by an unpaired two-tailed Student's *t*-test ($p = 0.4125$ [*sISP1*-KD],

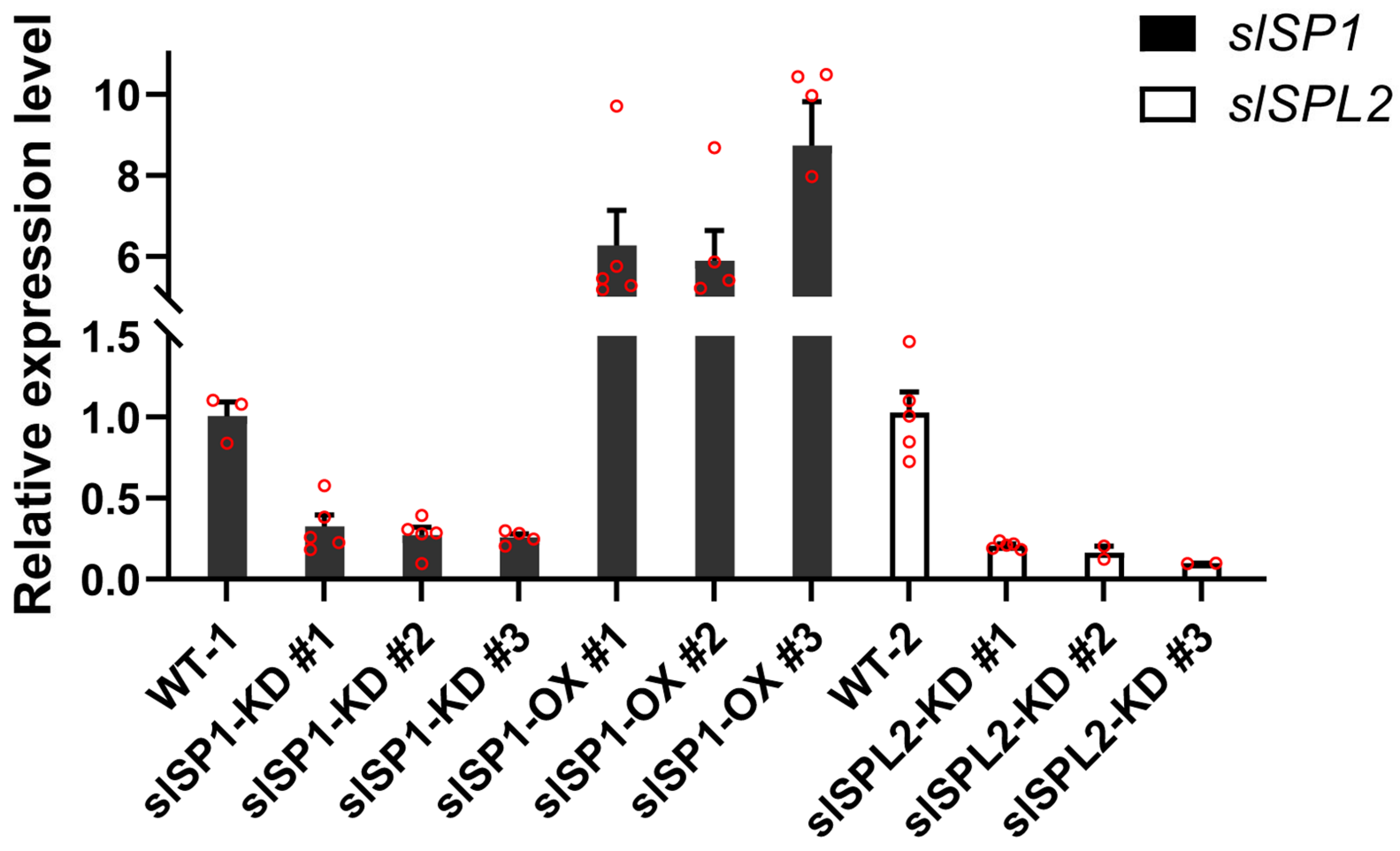
0.7132 [slSP1-OX], and 0.8001 [slSPL2-KD]). This rules out the possibility of nonspecific effects due to fruit size differences, which is important because ripening in detached tomato fruit is dependent on proper maturation up to the mature green stage¹⁷.

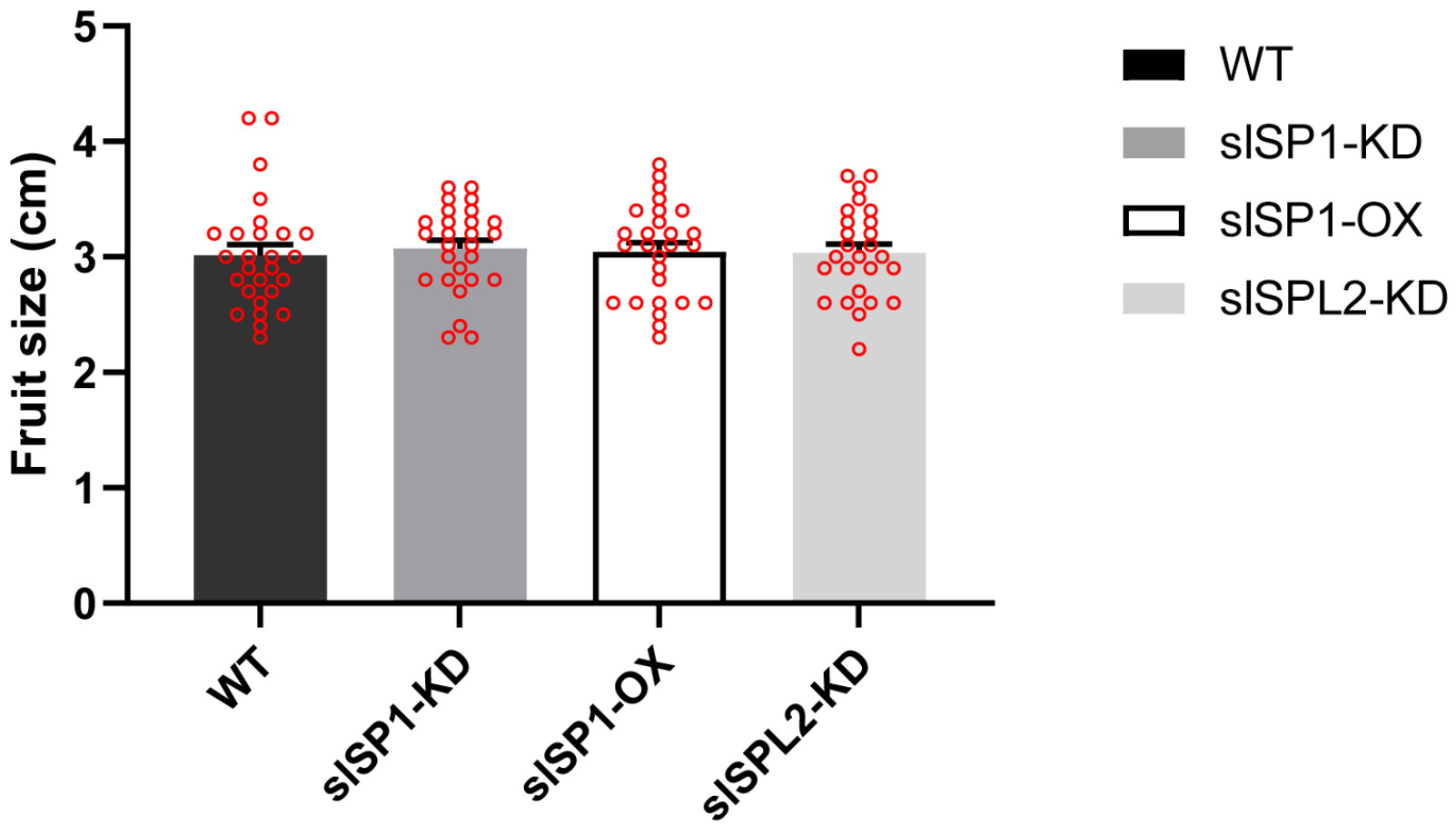
Extended Data Fig. 4 | Determination of firmness of detached tomato fruits. Fruit firmness was measured using a durometer at the breaker (Day 1) and red stages (**a**) ($n = 20-28$ [breaker stage] or 10-13 [red stage] fruits per genotype); or at specific days post breaker stage (**b**) ($n = 20-28$ [Day 1, Day 5, Day 9], 10-13 [Day 12], or 10-12 [Day 14] fruits per genotype). Note that slSP1-OX fruit at Day 14 were too soft to give a reading using the durometer. All values are means \pm SEM. The fruit used in this analysis were randomly chosen from the fruit populations of T2 generation plants used in the ripening analysis in Figure 3.

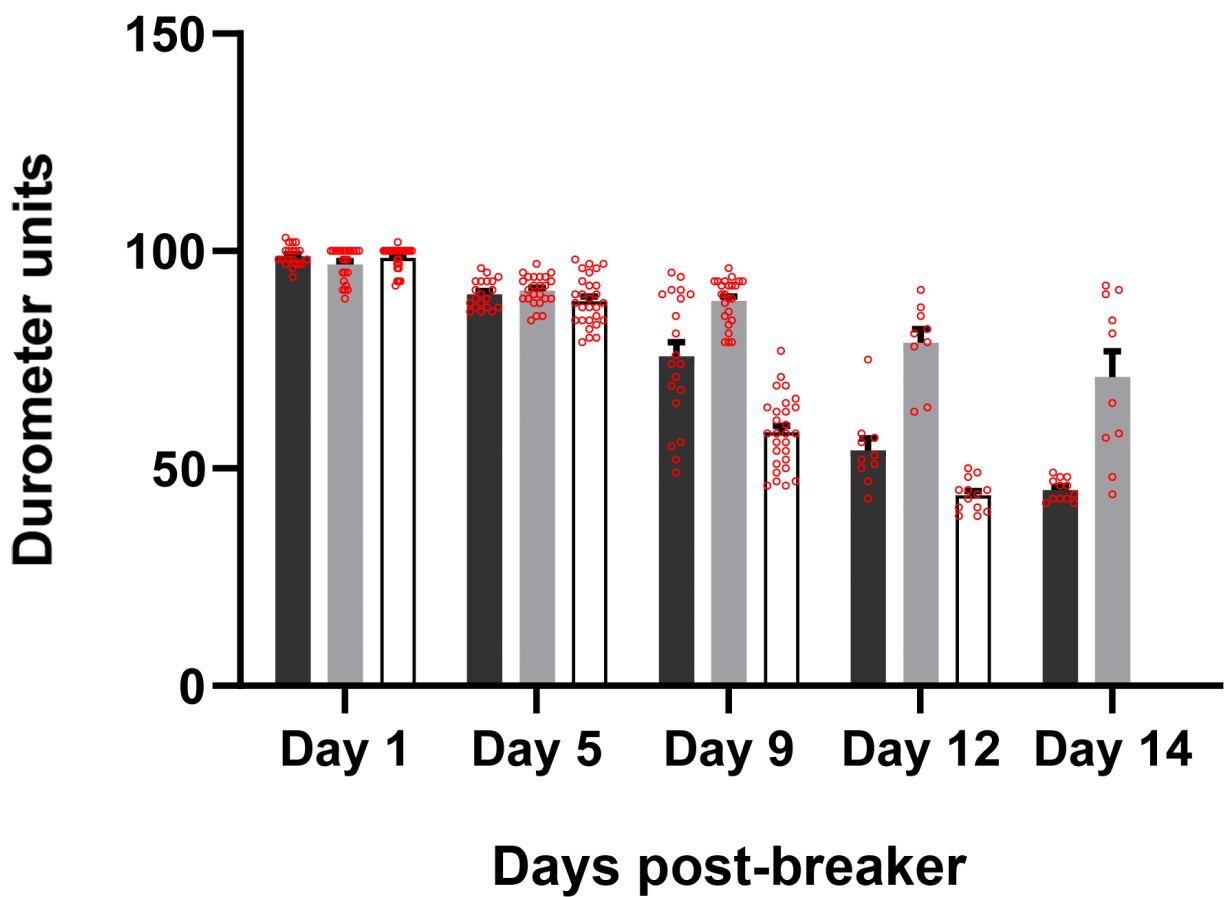
Extended Data Fig. 5 | Analyses of the effects of slSP1 on ripening-related gene expression. Total fruit RNA was extracted from wild-type (WT), slSP1-KD (KD), and slSP1-OX (OX) tomato plants at the Day 8 post-breaker stage (Day 8) stage and the red stage (the same fruit as those used in Figure 6). Relative mRNA expression levels were analysed by qRT-PCR using primers specific for genes involved in ethylene synthesis (**a**), cell wall modification (**b**), carotenoid biosynthesis (**c**), and master, ripening-related transcription factors (**d**). It was reported previously that all of these ripening-related genes are upregulated during fruit ripening; typically, in wild-type fruit, their transcript levels will reach a peak at the pink stage, and then reduce at the red stage³⁵⁻³⁷. Correspondingly, in our analysis, wild-type fruit at the Day 8 post-breaker stage (pink-looking) show higher expression levels than fruit at the red stage. Although the slSP1-KD and slSP1-OX fruits both showed similar lower mRNA levels of ripening-related genes at the red stage, at Day 8 they showed striking differences in mRNA levels. In general, slSP1-KD fruit (green-looking) had markedly reduced mRNA levels, while slSP1-OX fruit (red-looking) had gene expression levels in between those of wild-type and slSP1-KD fruits. Overall, these results indicated that slSP1-KD fruit show delayed transcriptional changes of ripening-related genes relative to wild-type fruit, whereas slSP1-OX fruit displayed accelerated transcriptional changes relative to wild-type fruit. Expression data for the genes of interest were normalized using data for the reference gene, *sLACTIN*. All values are expressed relative to the corresponding value for wild type, which in each case is set to 1. Values are means \pm SEM of three replicates. *ACO1*, 1-Aminocyclopropane-1-carboxylate oxidase 1; *ACS2/4*, 1-

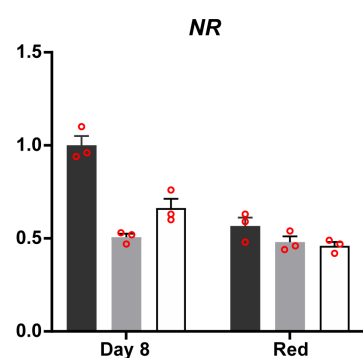
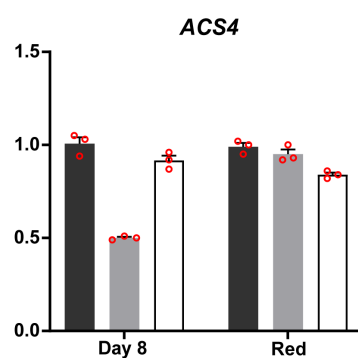
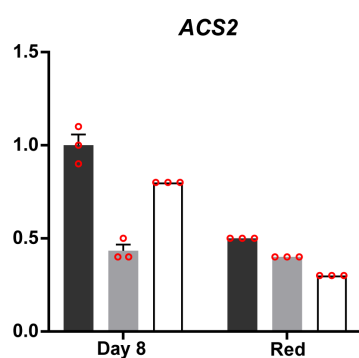
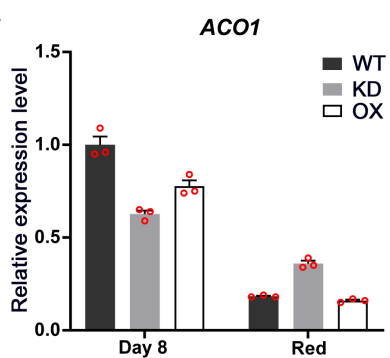
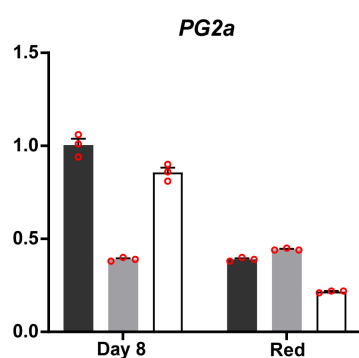
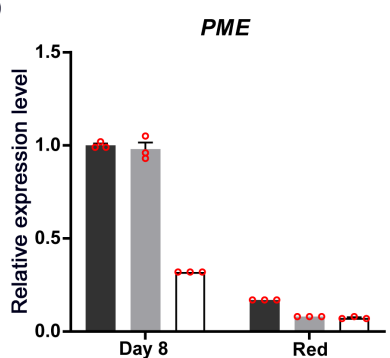
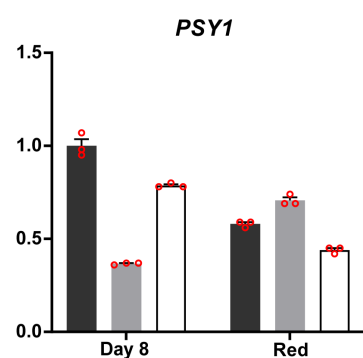
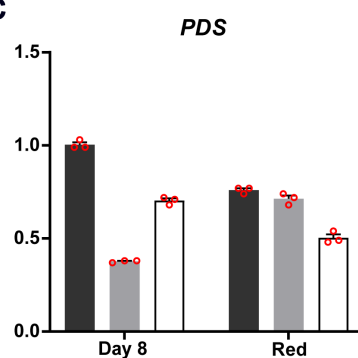
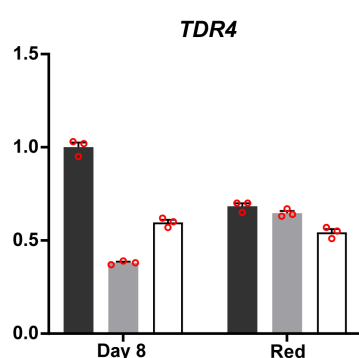
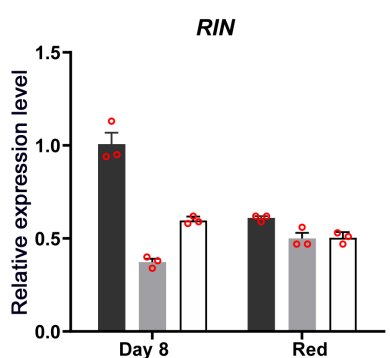
Aminocyclopropane carboxylic acid synthase 2/4; NR, Never ripe; PME, Pectin methylesterase; PG2a, Polygalacturonase 2a; PDS, Phytoene desaturase; PSY1, Phytoene synthase 1; RIN, Ripening inhibitor; TDR4, Agamous-like MADS-box protein AGL8 homolog.







a**b**

a**b****c****d**

Supplementary Table 1 | Primers used during the course of the study.

a, Primers used to generate various constructs.

Primer name	Primer sequence (5' to 3')	Used to generate ...
AttB1-SP1-F	AAAAAGCAGGCTCCACCGGAAATGGTTCCATG	... <i>slSP1</i> CDS, for the slSP1-OX construct, and for the C-terminal YFP fusion [NS: no stop codon]
AttB2-SP1-R	AGAAAGCTGGGTTTCAATGGCGAAAAGTTTTTCAC	
slSP1-NS-R	AGAAAGCTGGGTTATGGCGAAAAGTTTTTCACAAC	
slSPL2-F	AAAAAGCAGGCTCCATGTCAATATACGATCAAGCGG	... <i>slSPL2</i> CDS, for the C-terminal YFP fusion
slSPL2-NS-R	AGAAAGCTGGGTTTAACACACAGCGCTGGCA	
A-attB1	ACAAAAAGCAGGCTCTGCAAGGCGATTAAGTTGGGTAAC	... complete Gateway recombination sites for cloning into pDONR201
B-attB2	ACAAGAAAGCTGGGTGCGGATAACAATTTTCACACAGGAAACAG	

b, amiRNA target sequences.

Genes	Target sequence (5' to 3')	Positions
<i>slSP1</i>	TCATATGACCACACGCGACAA	917-937
	TAAGTAGATATACACTGACAG	698-718
<i>slSPL2</i>	TTGGCGTACGGAGTATTGTCA	92-112
	GAGACAGTTTATCATCACTTA	562-582

c, Primers used to amplify the coding sequences of the amiRNAs.

Primer name	Primer sequence (5' to 3')*	Gene
solSP1-AmR-1-I	gaTCATATGACCACACGCGACAAAtctctctttgtattcc	<i>slSP1</i>
solSP1-AmR-1-II	gaTTGTCGCGTGTGGTCATATGAtcaaagagaatcaatga	
solSP1-AmR-1-III	gaTTATCGCGTGTGGACATATGTtcacagtcgtgatatg	
solSP1-AmR-1-IV	gaACATATGTCCACACGCGATAAAtctacatatattcct	

solSP1-AmR-2-I	gaTAAGTAGATATACTGACAGtctctctttgtattcc	
solSP1-AmR-2-II	gaCTGTCAGTGTATATCTACTTAtcaaagagaatcaatga	
solSP1-AmR-2-III	gaCTATCAGTGTATAACTACTTTtcacaggtcgtgatatg	
solSP1-AmR-2-IV	gaAAAGTAGTTATACTGATAGtctacatatattcct	
solSPL2-AmR-92-I	gaTGACAATACTCCGTACGCCAAtctctctttgtattcc	<i>slSPL2</i>
solSPL2-AmR-92-II	gaTTGGCGTACGGAGTATTGTCAtaaagagaatcaatga	
solSPL2-AmR-92-III	gaTTAGCGTACGGAGAATTGTCTtcacaggtcgtgatatg	
solSPL2-AmR-92-IV	gaAGACAATTCTCCGTACGCTAAtctacatatattcct	
solSPL2-AmR-562-I	gaTAAGTGATGATAAACTGTCTCtctctctttgtattcc	
solSPL2-AmR-562-II	gaGAGACAGTTTATCATCACTTAtcaaagagaatcaatga	
solSPL2-AmR-562-III	gaGAAACAGTTTATCTTCACTTTtcacaggtcgtgatatg	
solSPL2-AmR-562-IV	gaAAAGTGAAGATAAACTGTTTcctacatatattcct	

* Nucleotides shown in lower case do not correspond to the target gene, but instead correspond to linker sequences or mutation sites.

d, Primers used in qRT-PCR experiments.

Primer name	Primer sequence (5' to 3')	Gene
solACT-F	TTGCTGACCGTATGAGCAAG	<i>slACTIN</i>
solACT-R	GGACAATGGATGGACCAGAC	
solSP1-F1	ATGGTTCCATGGGCCGGACTCTC	<i>slSP1</i>
solSP1-R1	TCAATGGCGAAAAGTTTTCAC	
solSP1-F2	TGCTGTCGGTGTATATCTACTTGT	
solSP1-R2	CTTCATCCTCATCTCCTGCTCTT	
solSPL2-F1	ATGTCAATATACGATCAAGCGG	<i>slSPL2</i>
solSPL2-R1	GCTCGTCAAGAATCATATATCC	
solSPL2-F2	TACGGAGTATTGTCAAGTTCA	
solSPL2-R2	CTATCAGAGTTGTGCGGAAGA	
solACO1-F	TTGAAGCAATGAAGGCAATGGAA	<i>slACO1</i> (Solyc07g049530)

solACO1-R	AACTTTATTCTACCATACATAAGAAGAGCA	
solACS2-F	CGTTTGAATGTCAAGAGCCAGG	<i>slACS2</i> (Solyc01g095080)
solACS2-R	TCGCGAGCGCAATATCAAC	
solACS4-F	AAATCTCCACCTTCACTAACGAAC	<i>slACS4</i> (Solyc05g050010)
solACS4-R	CCTAAGTCCTTGGAAGACTAGACAC	
solNR-F	CTCCCAGAGGCAGATTGAAC	<i>slNR</i> (Solyc09g075440)
solNR-R	TTCACAGACATCCCACCATC	
solPME-F	ATCCTAGGGTGGTGGCAGT	<i>slPME</i> (Solyc12g098340)
solPME-R	TGTCTTCCTTGAACATCCCA	
solPG2a-F	TCAAGGGCACAAGTGCAACAAAGG	<i>slPG2a</i> (Solyc10g080210)
solPG2a-R	TGCACGTAGCCTCTGATGGTTT	
solPDS-F	AGCAACGCTTTTTCTGATG	<i>slPDS</i> (Solyc03g123760)
solPDS-R	TCGGAGTTTTGACAACATGG	
solPSY1-F	ACAGGCAGGTCTATCCGATG	<i>slPSY1</i> (Solyc03g031860)
solPSY1-R	AGCTCAATTCTGTCACGCCT	
solRIN-F	GCTAGGTGAGGATTTGGGACAA	<i>slRIN</i> (Solyc05g012020)
solRIN-R	AATTTGCCTCAATGATGAATCCA	
solTDR4-F	ACTGGACTCTCCTCACCTTGGGG	<i>slTDR4</i> (Solyc06g069430)
solTDR4-R	AGCTGCACCTTGCTGCTGTGA	

Figure 6a

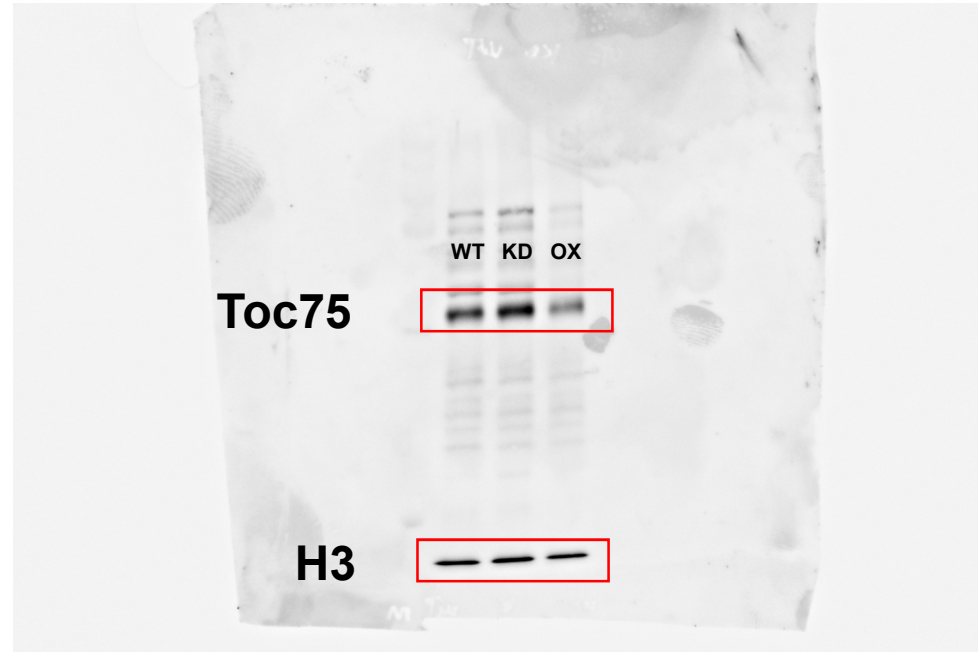


Figure 6a

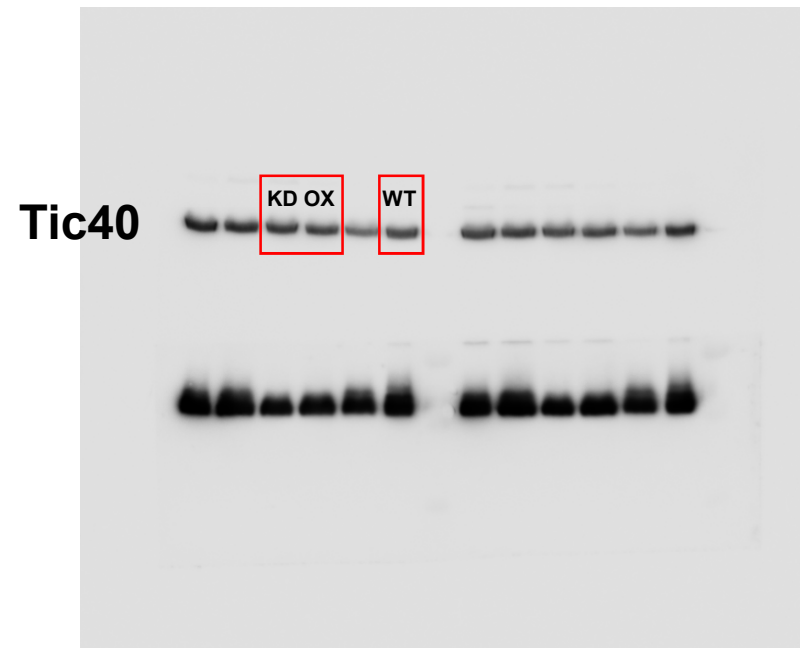


Figure 6c

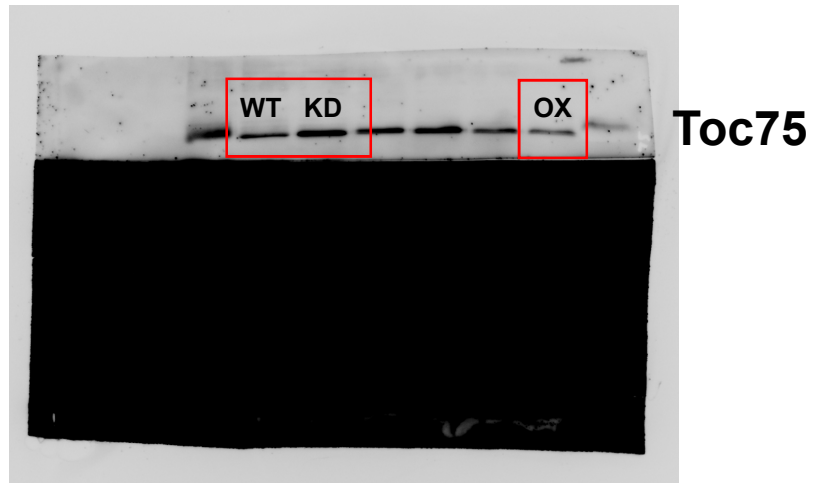


Figure 6c

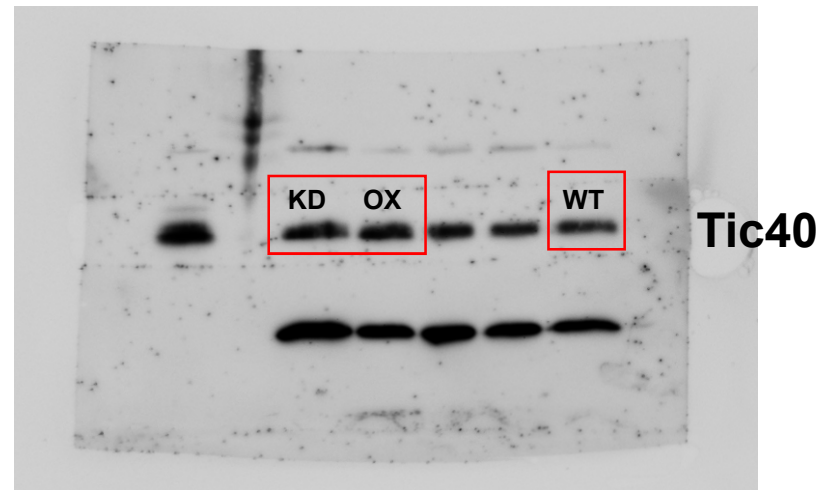


Figure 6c

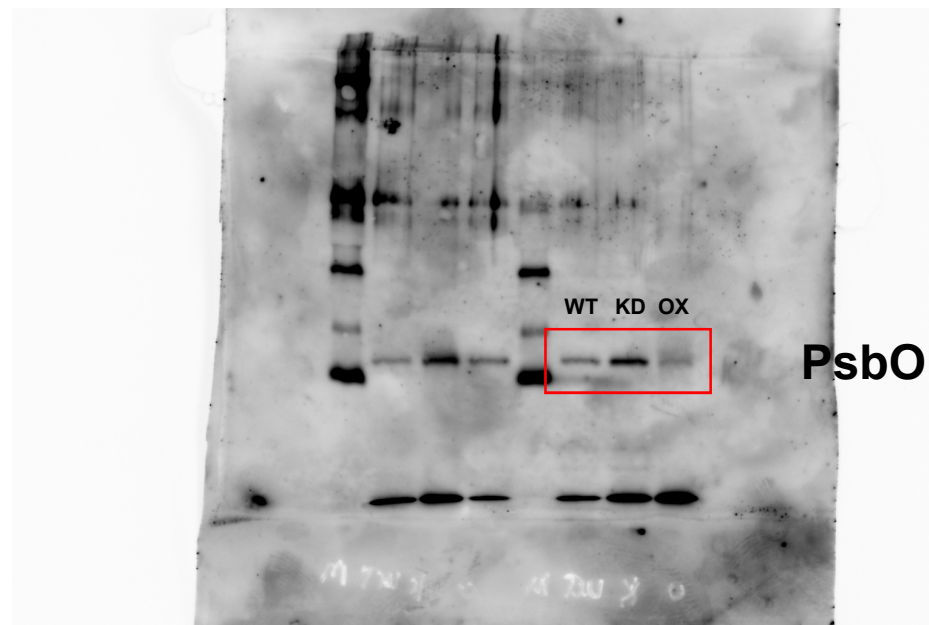


Figure 6c

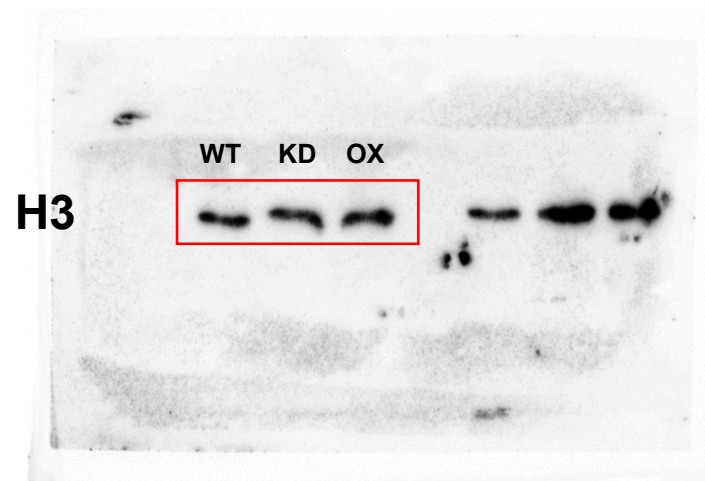


Figure 6e

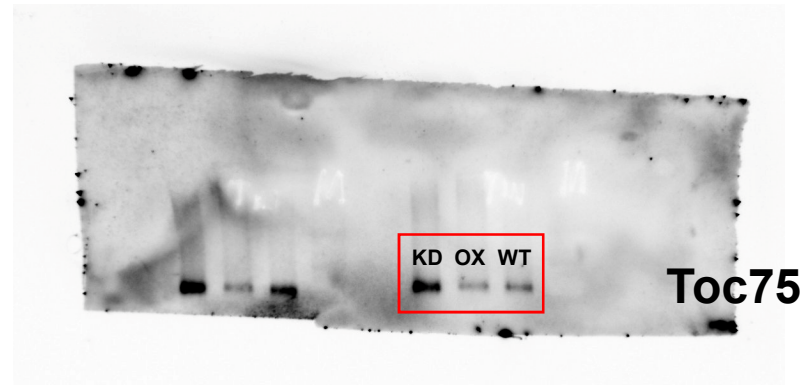


Figure 6e

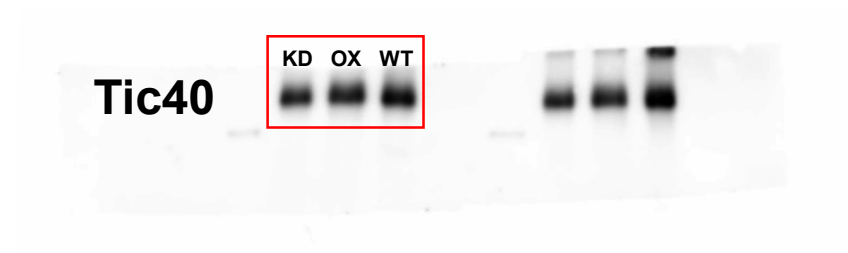


Figure 6e

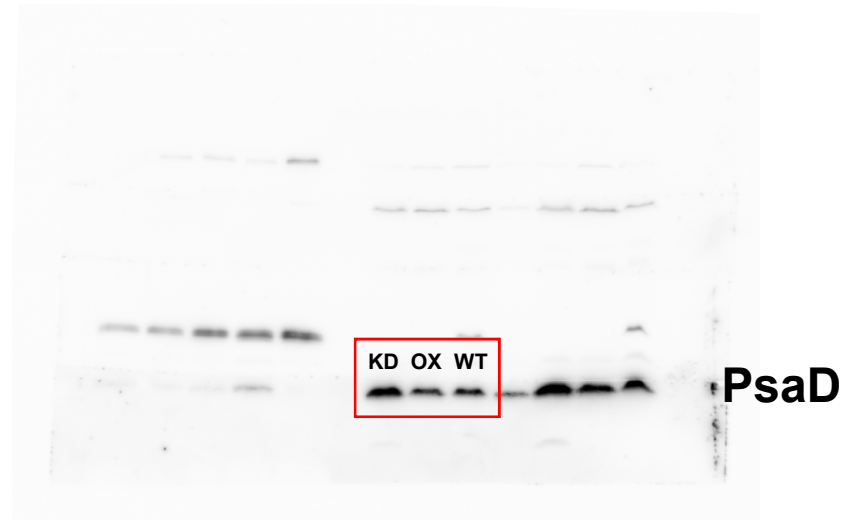


Figure 6e

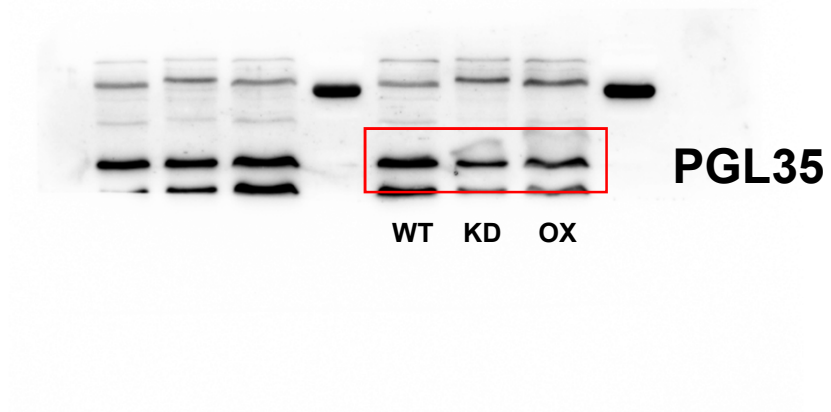


Figure 6e

